การควบคุมแบบสัมพรรคเป็นช่วงสำหรับรถจักรยานไร้คนขับโดยใช้การควบคุมคันบังคับ
และการรักษาเสถียรภาพด้วยผลของไจโรสโคป


นายปรัชญา รุ่งทวีสุข


วิทยานิพนธ์นี้เป็นส่วนหนึ่งของการศึกษาตามหลักสูตรปริญญาวิศวกรรมศาสตรมหาบัณฑิต

สาขาวิชาวิศวกรรมไฟฟ้า ภาควิชาวิศวกรรมไฟฟ้า

คณะวิศวกรรมศาสตร์ จุฬาลงกรณ์มหาวิทยาลัย

ปีการศึกษา 2554

ลิขสิทธิ์ของจุฬาลงกรณ์มหาวิทยาลัย

PIECEWISE AFFINE CONTROL FOR UNMANNED BICYCLE
USING STEERING CONTROL AND GYROSCOPIC STABILIZATION

Mr. Prachya Rungtweesuk

A Thesis Submitted in Partial Fulfillment of the Requirements
for the Degree of Master of Engineering Program in Electrical Engineering
Department of Electrical Engineering
Faculty of Engineering
Chulalongkorn University
Academic Year 2011

Thesis Title        PIECEWISE AFFINE CONTROL FOR UNMANNED BICYCLE
                    USING STEERING CONTROL AND GYROSCOPIC STABILIZATION

By                  Mr. Prachya Rungtweesuk

Field of Study      Electrical Engineering

Thesis Advisor      Assistant Professor Manop Wongsaisuwan, Ph.D.

---

Accepted by the Faculty of Engineering, Chulalongkorn University in Partial Fulfillment of the Requirements for the Master's Degree

. . . . . . . . . . . . . . . . . . . . . . . . . . . . . . . . . . . . . . . . . . . . . . . . . . . Dean of the Faculty of Engineering

(Associate Professor Boonsom Lerdhirunwong, Dr. Ing.)

THESIS COMMITTEE

. . . . . . . . . . . . . . . . . . . . . . . . . . . . . . . . . . . . . . . . . . . . . . . . Chairman

(Professor David Banjerdpongchai, Ph.D.)

. . . . . . . . . . . . . . . . . . . . . . . . . . . . . . . . . . . . . . . . . . . . . . . . Thesis Advisor

(Assistant Professor Manop Wongsaisuwan, Ph.D.)

. . . . . . . . . . . . . . . . . . . . . . . . . . . . . . . . . . . . . . . . . . . . . . . . External Examiner

(Itthisek Nilkhamhang, Ph.D.)

ปรัชญา รุ่งทวีสุข: การควบคุมแบบสัมพรรคเป็นช่วงสำหรับรถจักรยานไร้คนขับโดยใช้การควบคุมคันบังคับ และการรักษาเสถียรภาพด้วยผลของไจโรสโคป. (PIECEWISE AFFINE CONTROL FOR UNMANNED BICYCLE USING STEERING CONTROL AND GYROSCOPIC STABILIZATION) อ. ที่ปรึกษา วิทยานิพนธ์หลัก: ผศ.ดร. มานพ วงศ์สายสุวรรณ, 64 หน้า.


วิทยานิพนธ์ฉบับนี้นำเสนอการออกแบบรถจักรยานไร้คนขับที่สามารถตั้งอยู่ได้ในขณะที่เคลื่อนที่ไปตามทางได้เองโดยการจำลองผลด้วยคอมพิวเตอร์ รถจักรยานประกอบด้วยระบบหลักสองระบบ ได้แก่ ระบบรักษาเสถียรภาพและระบบนำทาง เราออกแบบแต่ละระบบแยกกันและนำมารวมเข้าด้วยกัน สำหรับระบบรักษาเสถียรภาพ เราพัฒนาวิธีใหม่ซึ่งใช้ทั้งการรักษาเสถียรภาพด้วยผลของไจโรสโคปและการควบคุมคันบังคับ เราออกแบบตัวควบคุมป้อนกลับสถานะซึ่งรับประกันเสถียรภาพของระบบไม่เชิงเส้นภายในบริเวณย่านการทำงานที่ต้องการและรับประกันสมรรถนะของระบบวงปิดในทางปฏิบัติบางชนิด เราประยุกต์กลยุทธ์ของระบบสัมพรรคเป็นช่วงเข้ากับวิธีกำหนดย่านการวางโพลและวิธีคุมค่ากำลังสองเชิงเส้น โดยการกำหนดวิธีออกแบบทั้งหมดได้ถูกเปลี่ยนให้เป็นปัญหาการหาค่าเหมาะสมของอสมการเมทริกซ์เชิงเส้น ตัวควบคุมแบบเวลาวิยุตหาได้จากตัวควบคุมแบบเวลาต่อเนื่องโดยวิธีการอสมการเมทริกซ์เชิงเส้นเช่นกัน สำหรับระบบนำทาง เราออกแบบตัวควบคุมโดยการประยุกต์การถดถอยเชิงเส้นโดยใช้วิธีความผิดพลาดกำลังสองน้อยสุด จากนั้นระบบที่รวมระบบรักษาเสถียรภาพและระบบนำทางได้ถูกออกแบบขึ้น เรานำเสนอขั้นตอนสำหรับการคำนวณค่ามุมคันบังคับที่ต้องการใหม่ ผลการจำลองด้วยคอมพิวเตอร์แสดงให้เห็นประสิทธิผลของวิธีการออกแบบที่นำเสนอ

ภาควิชา .......... วิศวกรรมไฟฟ้า .......... ลายมือชื่อนิสิต ..........

สาขาวิชา .......... วิศวกรรมไฟฟ้า .......... ลายมือชื่อ อ.ที่ปรึกษาวิทยานิพนธ์หลัก ..........

ปีการศึกษา .......... 2554 ..........

# # 5470264621 : MAJOR ELECTRICAL ENGINEERING

KEYWORDS : UNMANNED BICYCLE / GYROSCOPIC STABILIZATION / STEERING CONTROL / PIECEWISE AFFINE SYSTEM / LINEAR MATRIX INEQUALITIES

PRACHYA RUNGTWEESUK : PIECEWISE AFFINE CONTROL FOR UNMANNED BICYCLE USING STEERING CONTROL AND GYROSCOPIC STABILIZATION. ADVISOR : ASST. PROF. MANOP WONGSAISUWAN, Ph.D., 64 pp.


This thesis presents the design of an unmanned bicycle that can stay upright while following the path autonomously in a computer simulation. The bicycle consists of two main systems; stabilization system and navigation system. We design each system separately and combine them together. For the stabilization system, we develop a novel technique which utilizes both the gyroscopic stabilization and the steering control. We design a state-feedback controller which guarantees the stability of a class of nonlinear systems over the desired operating region and ensures some practical performance criteria of the closed-loop system. We apply the piecewise affine technique together with the regional pole placement and linear quadratic regulator in order that all design formulations are cast as a linear matrix inequalities (LMI) optimization problem. The discrete-time controller is also obtained from the continuous-time controller via LMI approach. For the navigation system, we design a controller by applying a linear regression using least square error method. Then an integrated stabilization and navigation system of the bicycle has been designed. We propose the algorithm for recalculating the desired steering angle. The simulation results illustrate the effectiveness of the proposed design methods.

Department : ...Electrical Engineering...    Student's Signature .......................

Field of Study : ...Electrical Engineering...    Advisor's Signature .......................

Academic Year : .........2011...........

# Acknowledgements

First and foremost, I would like to express my sincere gratitude to my thesis advisor, Assistant Professor Manop Wongsaisuwan, for his supervision and guidance. He gave me useful advices and allowed me the latitude to do my research in various directions. He also provided me an opportunity to attend an overseas conference and helped me improve my English skills. It is a great and invaluable experience for me to work with him.

I would like to thank Associate Professor David Banjerdpongchai and Dr. Jitkomut for providing me essential knowledge for this research. I also express my thankfulness to my thesis committees, Associate Professor David and Associate Professor Itthisek Nilkhamhang who had given constructive suggestions for the improvement in my research.

Many thanks to all colleagues, especially, Sompol Suntharasantic who initiates a piecewise affine control for the experimental bicycle, Pakorn Sukprasert for his effort implementing electrical system on the bicycle, Parunya Taranajetsada for her suggestion in mechanical aspect. This thesis could not be successfully completed without their kindness. Thanks also to all members of Control Systems Research Laboratory (CSRL) who have offered me an enjoyable work environment, former CSRL members who created the latex class for this thesis. I greatly appreciate the financial support from the Electrical Engineering Department, Chulalongkorn University.

Finally, I would like to thank my parents for their support during my study and their encouragements that help me go through the hard times.

# Contents

# List of Tables

# List of Figures

# CHAPTER I

# INTRODUCTION

## 1.1 Research motivation

The first two-wheel vehicle has been built by Macmillan in 1839 and it was developed for more comfortable and safer along this century until it looked similar to the modern bicycle. The bicycle is an environmentally friendly vehicle because it doesnt emit any air pollution. It also can move through narrow streets conveniently compare to a car. The bicycle was the popular transportation just prior to the automobile in late 19th century. However, it is the modern concerns around global warming and could lead the bicycle to once again becoming the worldwide transportation.

The bicycle control is one of a challenge problem in a field of control. The bicycle robot has received much attention in the past few decades. In recent years, Thai Robotics Society organizes the Bicyrobo Thailand Championship competition in order to provide the opportunity to develop the bicycle control technology. Several students from all universities in Thailand, including us, have attended this competition. So this is the beginning of the bicycle project. We design the bicycle control system that utilizes both steering control and gyroscopic stabilization since we expect that the combination of available bicycle control techniques should give the better result. Then we simulate the result via computer simulation in this thesis.

Piecewise Affine (PWA) Systems are defined by a series of linear subsystems. They can describe dynamics involving both continuous and discrete behaviors of hybrid system and approximate nonlinear systems. So PWA systems are well-known structure. The main advantage of PWA systems is that they provide a systematic approach to handle the nonlinear control design problem while maintaining the simplicity of linear system. Moreover, we design the controller in LMI approach because various design techniques can be combined by using LMI.

## 1.2 Literature review

The literature review will be separated into two parts including: a bicycle dynamic & control part and a piecewise affine control part.

### 1.2.1 Bicycle dynamic & control

In the 19th century, the studies of bicycle dynamic have arisen and became a popular topic in late of this century. The first correct linearized equation of motion for the bicycle was found in 1899 by Whipple [1]. The nonlinear equation was derived based on Lagrange mechanic but some

constraints were missing. Many models were also derived based on Lagrange mechanic in [2], [3], [4], [5]. Some simple models were derived based on Newton's law in order to capture only some major effects on the bicycle [6]. When the computing facilities were available, the more complicated models [7], [8] were obtained using software for multi-body system. The software, such as Sophia [8] Modelica [9] and Autosim [10], view the mechanical system as an interconnection of subsystem. The order of obtained nonlinear model is depend on the prior assumptions. Each assumption has been researched. For example, Roland [11] introduced side slipping and force generated from tires into the model, Limbeer and Sharp [12] toke the tire deflation and flexible frame into account, Jones [13] and Sharp [14] found that the design of the front fork has a major impact for self-stabilization, Jones [13] and Sommerfeld [15] summarized that the gyroscopic effect of the wheels are very small compared with the centrifugal effects at normal speed, etc. The good summary and history of bicycle dynamic can be found in Limebeer [12], Åström [16] and TU Delft [17].

The bicycle robot has received much attention in the past few decades. Although the bicycle can be self-stable but it must move with very specific speed interval. So the addition actuator should be installed for stabilizing the bicycle. There are three major techniques for the bicycle stabilization: Using the centrifugal force by steering control [18], [19], Using the balancer to shift the center of gravity of overall bicycle like a leaning of rider [2], Using the gyroscopic effect by controlling the gyroscopic flywheel [4], [20], [21], [22]. Some papers use the combination of these techniques such as [5] combined balancer with steering control and [23] can switch the actuator to be either flywheel or balancer. Note that we have never found the research which combined both steering and gyroscopic stabilization as our work. In addition some works [2] focus on the navigation system for the intelligent bicycle robot. Furthermore, several control design methods have been done on the bicycle such as input-output linearization [3], output zeroing [5], fuzzy-sliding mode control [24], backstepping design [25], LQR [26], sliding mode control [27] etc.

### 1.2.2 Piecewise affine control

Piecewise Affine (PWA) systems are categorized into a class of nonlinear system and a kind of hybrid system which unifies the framework for describing dynamics involving both continuous and discrete behaviors. They are defined by a series of affine subsystems. A switching among various affine models occurs when the state moves across the partition of each region. Sometimes PWA systems are also called as Piecewise Linear (PWL) System. But some papers define PWL systems as a series of linear subsystems. PWA systems are equivalent to another type of models such as mixed logical dynamical systems [28], max-min-plus-scaling systems [29]. This result allows extending all of the techniques developed for PWA models to another system. Moreover, due to the universal approximation property [30] of PWA systems, which means any nonlinear system can be approximated by PWA systems with desired accuracy, PWA systems are well-known structures and have been developed for analysis and control design of both nonlinear systems and hybrid systems.

During 1950s, the field of nonlinear network has received intense attention since the linear system theory was developed to meet its best performance such as optimum linear filter. PWA system is the powerful technique which can be used to approximate the nonlinear systems and also maintain the simplicity of linear systems. The first work on piecewise linear model can be traced back to [31] that represented the nonlinear resistive network in order to find the solution of the analysis problem. The systematic algorithm of PWA technique was proposed in [32]. At the beginning, many researches on PWA consider the model structure and their useful properties. Chua presented a Canonical PWL representation in explicit form [33], [34], [35] and used it to model the electronic devices [36], [37]. Lin [30] proved the universal properties of CPWL approximation and Julian [38] generalized CPWL representation for multivariable.

From the analysis problem to the control design problem, all paper contributions relating PWA focus on two issues: the modeling of PWA system and the controller design for PWA system. For the first issue, some researchers consider the continuous-time model such as approximating by sum of hinging hyperplanes [39], [40], sum of hinging sigmoid functions [41], series of linearized models at the appropriate vertices [42], applying Newton-Gauss algorithm [43], solving with mixed integer linear programming solver [44], [45], while some researchers consider the identification method of discrete-time model in state space model [46] and PWA autoregressive exogenous (PWARX) model. Numerous techniques were proposed, for instance, linear regression based on least square method [47], [48], a cluster technique which classifying the data into different groups before estimating the models [47], Bayesian procedure for modelling parameters as the random variables [49], bounded-error procedure [50]. These four procedures have been compared in [51], and a good overview of identification of hybrid system can be founded in [52]. For the second issue, Sontag [53] proposed the asymptotic properties and controller design for PWA systems which was the first step in the development of controller design for PWA systems. The observability and controllability of PWA systems have been proposed in [28], then the observer design in [54] and the observer-based control in [55], [56]. To guarantee the stability of PWA systems, Hassibi and Boyd proposed a method based on finding the continuous piecewise quadratic Lyapunov function in [57] but [58] showed that the continuity of the Lyapunov function is not required in the discrete time case. These problems can be formulated into LMI problems and solved by available solvers [59], [60]. Ran and Johansan extended the stability analysis to the performance analysis and optimal control in [61] and summarized the controller synthesis containing with BMI approach in [62]. Furthermore, MPC design method was adopted for PWA systems in [29], [63].

Since incorporating linear matrix inequality (LMI) or bilinear matrix inequality (BMI) or model predictive control (MPC) to deal with control design problem give a systematic approach to handle the nonlinear control design problems, there are several applications which take this advantage in [63], [64], [65].

In this thesis, we continue to work on the PWA controller design closely with Sompol, a for-

mer student, in [66] which left the performance design and the implementation on the prototype of experimental bicycle for further development.

## 1.3   Thesis objective

The main objective of this research is to design a state-feedback controller which guarantees the stability of a class of nonlinear systems over the desired region and ensures some practical performance criteria of the closed-loop system. We apply the piecewise affine technique together with the regional pole placement and linear quadratic regulator in order that all design formulations are cast as a linear matrix inequalities optimization problem. The discrete-time controller is also obtained from the continuous-time controller via LMI approach. An integrated stabilization and navigation system of an intelligent bicycle robot has been design. Moreover, we develop a novel stabilization technique which utilizes not only the gyroscopic stabilization but also incorporating the steering control for the intelligent bicycle robot in the computer simulation.

## 1.4   Scope of thesis

1. To develop a stabilization technique which utilizes both steering control and gyroscopic stabilization.

2. To synthesize the state-feedback controller based on piecewise affine technique that ensures some practical performance criteria of the closed-loop system.

3. To design an intelligent bicycle robot which can stay upright while following the path in the computer simulation.

## 1.5   Methodology

1. Conduct the literature review on a bicycle model and PWA systems.

2. Derive a bicycle model which utilizes both steering control and gyroscopic stabilization.

3. Design a controller for stabilizing the unmanned bicycle by employing PWA technique.

4. Design a navigation system for tracking the desired path.

5. Integrate the stabilization system and the navigation system.

6. Find the practical parameters from some experiments.

## 1.6   Contributions

1. A piecewise affine controller for an unmanned bicycle using gyroscopic stabilization.

2. A novel stabilization technique which combine both steering and gyroscopic stabilization for the unmanned bicycle.

## 1.7   Thesis outline

The organization of the thesis is as follows. Chapter 2 introduces an essential background knowledge that relates with the proposed controller design method. Chapter 3 presents the system model of the bicycle. Chapter 4-5 present the controller design for stabilization system and navigation system respectively. The integration of both system has been shown in chapter 6. Finally, we give the conclusion and future work guideline in the last chapter.

# CHAPTER II

# RELATED THEORIES

## 2.1 Linear matrix inequality (LMI)

A linear matrix inequality (LMI) is a constraint of the form:

$$F(x) = F_0 + \sum_{k=0}^{\infty} x_i F_i > 0 \qquad ; x \in \mathbb{R}^m, F_i = F_i^T > 0 \in \mathbb{R}^{m \times m}$$

If the matrix inequality has the product terms between two variables but it is LMI when we fix one of them as a constant, this matrix inequality is called bilinear matrix inequality (BMI). The multiple LMIs, $F^{(i)}(x) > 0$ for all $i \in \{1, 2, ..., p\}$, can be formulated as a single LMI:

$$\text{diag}(F^{(1)}(x), ..., F^{(p)}(x)) > 0$$

Next, we introduce some useful properties of the LMI which related our controller design.

**Theorem 2.1.** Schur complement

*Given the matrices $Q(x) = Q(x)^T \in \mathbb{R}^{n \times n}, R(x) = R(x)^T \in \mathbb{R}^{m \times m}$ and $S(x) \in \mathbb{R}^{n \times m}$, which depend affinely on x. Then the LMI*

$$\begin{bmatrix} Q(x) & S(x) \\ S^T(x) & R(x) \end{bmatrix} > 0$$

*is equivalent to the following LMIs*

$$R(x) > 0, \qquad Q(x) - S(x)R(x)^{-1}S(x)^T > 0$$

*or*

$$Q(x) > 0, \qquad R(x) - S(x)^T Q(x)^{-1} S(x) > 0$$

**Theorem 2.2.** $S$-procedure for quadratic forms and nonstrict inequalities

*Let $Q_0(x), ..., Q_p(x)$ be quadratic functions of $x \in \mathbb{R}^n$,*

$$Q_i(x) = x^T A_i x + 2b_i^T x + c_i = \begin{bmatrix} x \\ 1 \end{bmatrix}^T \begin{bmatrix} A_i & b_i \\ b_i^T & c_i \end{bmatrix} \begin{bmatrix} x \\ 1 \end{bmatrix} \quad ; \text{ for all } i \in \{0, ..., p\}, A_i = A_i^T$$

*If there exists $\tau_1 \geq 0, ..., \tau_p \geq 0$ such that*

$$Q_0(x) - \sum_{i=1}^{p} \tau_i Q_i(x) \geq 0$$

*then the following condition holds*

$$Q_0(x) \geq 0 \quad \text{for all } x \quad \text{such that } Q_i(x) \geq 0 \quad \text{for all } i \in \{1, ..., p\}$$

Unfortunately, the converse of theorem 2.2 is in general false except for $p = 1$. Moreover, if we replace the non-strict inequalities by strict inequalities, the converse theorem in case $p = 1$ is also not true. This result may lead to the conservatism in our controller design approach. However, it appears to work very well in practice [62]

## 2.2 Piecewise affine system (PWA)

The Piecewise Affine system is a kind of nonlinear system which has its own linear dynamics in each local region. The advantage of PWA system is it can be used as a tool for extending several techniques of linear system to nonlinear system via approximated PWA system.

### 2.2.1 Model representation

In this thesis, we consider the continuous-time piecewise affine systems in state-space form:

$$\left.\begin{aligned} \dot{x} &= A_i x + a_i + B_i u \\ y &= C_i x + c_i \end{aligned}\right\} \quad x \in X_i \tag{2.1}$$

where $x$ is the state vector, $u$ is the control input, $i$ is the index of polyhedral region $X_i \subseteq \mathbb{R}^n$.

For convenience, we can rewrite the PWA model in a more compact form

$$\left.\begin{aligned} \dot{\bar{x}} &= \bar{A}_i \bar{x} + \bar{B}_i u \\ \bar{y} &= \bar{C}_i \bar{x} \end{aligned}\right\} \quad x \in X_i \tag{2.2}$$

where

$$\bar{x} = \begin{bmatrix} x \\ 1 \end{bmatrix}, \bar{A}_i = \begin{bmatrix} A_i & a_i \\ 0 & 0 \end{bmatrix}, \bar{B}_i = \begin{bmatrix} B_i \\ 0 \end{bmatrix}, \bar{C}_i = \begin{bmatrix} C_i & c_i \end{bmatrix}$$

Next, let us introduce two types of cell bounding for describing polyhedral region $X_i$

- Polyhedral cell bounding

  A polyhedral cell bounding is a matrix $\bar{E}_i = \begin{bmatrix} E_i & e_i \end{bmatrix}$ which $\bar{E}_i \bar{x}_i \succeq 0$ for all $x \in X_i$. Note that the notation $\succeq$ means greater than or equal for all vector elements.

- Ellipsoid cell bounding

  The ellipsoidal cell description can be written in form $\varepsilon = \{||S_i x + s_i||_2 \leq 1\}$. The parameters $(S_i, s_i)$ of the approximated ellipsoid bounding, which contains the polytope described by vertices $\{v_1, ... v_m\}$, can be computed by solving the convex optimization problem

$$\begin{aligned} \min_{S_i, s_i} \quad & \log \det S_i^{-1} \\ \text{subject to} \quad & \begin{bmatrix} I & S_i v_j + s_i \\ v_j^T S_i^T + s_i^T & 1 \end{bmatrix} \geq 0 \\ & S_i = S_i^T > 0 \quad \text{for } j = 1, ..., m \end{aligned} \tag{2.3}$$

### 2.2.2 Piecewise affine model approximation

There are several method for approximating the piecewise affine system. However, we use our own approximation method base on least square technique which have been proposed in [68] due to its simplicity. We start with defining the regions that will be approximated by PWA model. In fact, the defined boundary is selected to minimize the error of overall regions under some prior information such as the number of partition, the range of operating region and the form of partition. The more regions lead to more accurate model but more calculation is needed.

First, we linearize the nonlinear system around the operating point in order to make this region the most accurate and avoid the error of equilibrium point in the approximated model. Then, we can approximate the nearby region with 2 alternative methods:

- Least-square error approximation with discontinuous boundary

To obtain the PWA model, we formulate the least square problem from the approximated linear model of region $i$

$$y_{N \times 1} = G^{(i)}_{N \times (n+1)} \theta^{(i)}_{(n+1) \times 1} + \mu_{N \times 1} \tag{2.4}$$

where

$G^{(i)}$ is the state vector with affine term $\begin{bmatrix} x_1^{(i)} & ... & x_n^{(i)} & 1 \end{bmatrix}$

$\theta^{(i)}$ is the estimated plant parameters $\begin{bmatrix} \theta_1^{(i)} & ... & \theta_n^{(i)} & \theta_{n+1}^{(i)} \end{bmatrix}^T$

$y$ is the exact value of nonlinear function, i.e. $\ddot{\varphi}$ or $\ddot{\alpha}$ for the bicycle dynamic equation

$\mu$ is the approximation error

$x_k^{(i)}$ is the vector of $k^{th}$ state containing $N$ realizations of a uniform random variable in the range $[x_{k_{min}}, x_{k_{max}}]$ in each $X_i$

$N$ is the number of realization

Then we can present the problem as

$$\hat{\theta}^{(i)} = \underset{\theta^{(i)}}{\operatorname{argmin}} \left\| y - G^{(i)} \theta^{(i)} \right\|_2^2 \tag{2.5}$$

The closed form solution is

$$\hat{\theta}^{(i)} = (G^{(i)T} G^{(i)})^{-1} G^{(i)T} y \tag{2.6}$$

Since there is no constraint in the least square problem, we can approximate the system matrices for each region separately.

- Least-square error approximation with continuous boundary

Recall the least square problem (2.5). The additional constraints are taken into account when an approximation is done with the continuous boundary. The problem formulation for region $i$ becomes

$$\begin{aligned} \text{minimize} \quad & \left\| \ddot{y} - G^{(i)} \theta^{(i)} \right\|_2^2 \\ \text{subject to} \quad & G_\gamma^{(i,j)} \theta^{(i)} = G_\gamma^{(i,j)} \theta^{(j)} \text{ ; For all } X_j \text{ which connect to } X_i \end{aligned} \tag{2.7}$$

where $G_\gamma^{(i,j)}$ is the state vector with affine term $\begin{bmatrix} x_1 & ... & x_n & 1 \end{bmatrix}\Big|_{x_k=\gamma}$

for the common boundary of region $i$ and $j$ which describes by $x_k = \gamma$

Note that we can approximate all regions simultaneously in order to minimize the error of the overall region

## 2.3  Controller design via LMI

### 2.3.1  Quadratic stabilization

**Theorem 2.3.** Lyapunov stability

*Consider the autonomous nonlinear system $\dot{x} = f(x)$. If there exists a scalar Lyapunov function $V(x)$ which satisfy following conditions:*

(1)  $V(0) = 0$

(2)  $V(x) > 0 \, ; \, \forall x \neq 0$

(3)  $\dot{V}(x) < 0$

*Then, the equilibrium point $x_e = 0$ is asymptotically stable.*

There is no general method for searching the Lyapunov function. However, the task of finding the Lyapunov function for linear system is much more systematic with the prior assumption on lyapunov function. Fortunately, we can analyze the stability problem of nonlinear system around the equilibrium point from the linearized system that can be formulated as LMIs.

**Theorem 2.4.** Quadratic stability

*Consider the autonomous linear system $\dot{x}(t) = Ax(t)$, assume the Lyapunov function is $V(x) = x^T P x$, called quadratic lyapunov function. The equilibrium point $x_e = 0$ is asymptotically stable if there exists a symmetric matrix $P = P^T$ satisfying these LMIs*

$$
\begin{aligned}
P &> 0 \\
A^T P + PA &< 0
\end{aligned}
$$

(2.8)

*Proof.* Substitute the Lyapunov function directly into theorem 2.3. We get

$$\dot{V}(x) = \dot{x}^T P x + x^T P \dot{x} = x^T (A^T P + PA)x < 0$$

$\square$

For the controller synthesis purpose, we can apply theorem 2.4 by replacing system matrix A with close-loop system $A_{cl}$. However, the problem won't be the LMI problem but we can recover it as following theorem.

**Theorem 2.5.** Quadratic stabilization

*Suppose the linear system is $\dot{x} = Ax + Bu$. The closed-loop system is stable if there exist a*

*symmetric matrix $Y = Y^T$ and a matrix $W$ such that*

$$Y > 0$$

$$YA^T + AY - W^T B^T - BW < 0$$

(2.9)

*Then, the system can be stabilized by a state feedback controller $u = -Lx$ where $L = WY^{-1}$.*

*Proof.* From theorem 2.3, we replace $A$ with $A - BL$ and multiply both left and right with $P^{-1}$

$$P^{-1} = (P^{-1})^T > 0$$

$$P^{-1}(A - BL)^T + (A - BL)P^{-1} < 0$$

Then, change the variables $Y = P^{-1}$ and $W = LP^{-1}$. This completes the proof. $\square$

Note that the controller design of regional pole placement and LQR technique in another section are based on these theorems. Next, let us introduce the extension of previous stability analysis for piecewise affine system.

**Theorem 2.6.** Piecewise quadratic stabilization [62]

Given the PWA system $\dot{x} = A_i x + a_i + B_i u$ for $x \in X_i$ whose the region $X_i$ is contained in the ellipsoid $\{||S_i x + s_i||_2 \leq 1\}$. If there exist a positive definite matrix $Y = Y^T > 0$, positive scalars $v_i \geq 0$ and a matrix $W$ such that

$$YA_i^T + A_iY - W^T B_i^T - B_iW < 0 \quad ; \quad 0 \in X_i$$

$$\begin{bmatrix} YA_i^T + A_iY - (B_iW)^T - B_iW - v_i a_i a_i^T & YS_i^T - v_i a_i s_i^T \\ (YS_i^T - v_i a_i s_i^T)^T & v_i(I - s_i s_i^T) \end{bmatrix} < 0 \quad ; \quad 0 \notin X_i$$

(2.10)

*Then, the PWA system can be stabilized by a state feedback controller $u = -Lx$ where $L = WY^{-1}$.*

*Proof.* The first LMI is the result from theorem 2.5. For the second LMI, substitute the quadratic Lyapunov function directly into theorem 2.3 for closed-loop system. We get the LMI:

$$\begin{bmatrix} (A_i - B_iL)^T P + P(A_i - B_iL) & Pa_i \\ a_i^T P & 0 \end{bmatrix} < 0$$

And the ellipsoid cell bounding can be also written in LMI as

$$\begin{bmatrix} -S_i^T S_i & -S_i^T s_i \\ -s_i^T S_i & 1 - s_i^T s_i \end{bmatrix} \geq 0$$

By applying $S$-procedure, we obtain the LMI condition

$$\begin{bmatrix} (A_i - B_iL)^T P + P(A_i - B_iL) & Pa_i \\ a_i^T P & 0 \end{bmatrix} + \tau_i \begin{bmatrix} -S_i^T S_i & -S_i^T s_i \\ -s_i^T S_i & 1 - s_i^T s_i \end{bmatrix} < 0$$

Consider the system as norm-bound linear system. The quadratic stability can be interpreted as $H_\infty$ norm of the system is less than one. With a duality property of the system $\dot{x} = A_{cl}x + ap$, $q = Sx + sp$ and $\dot{x} = A_{cl}^T x + S^T p$, $q = a^T x + s^T p$, we get the LMIs in this theorem by changing the variables.

$\square$

However, it may be difficult to find a single Lyapunov function for all region especially when deal with the numerous constraints. To relax this problem, we can replace $Y$ with $Y_i$ to get the piecewise controller gain $L_i = WY_i^{-1}$ which can stabilize each local region.

### 2.3.2 Regional pole placement

The pole placement problem for any controllable system can be obtained from several well-known methods. We can design full state-feedback which yields the desired closed-loop poles. However, in many practical applications, the strict assignment is not necessary. So the regional pole placement has been introduced.

**Definition 2.1.** *Kronecker Product*

*Let $P = (p_{ij}) \in \mathbb{R}^{m \times n}$ and $Q = (q_{ij}) \in \mathbb{R}^{p \times q}$. Then the Kronecker Product of two matrices is defined as*

$$P \otimes Q = \begin{bmatrix} p_{11}Q & \cdots & p_{1n}Q \\ \vdots & \ddots & \vdots \\ p_{m1}Q & \cdots & p_{mn}Q \end{bmatrix} \in \mathbb{R}^{mp \times nq}$$

**Definition 2.2.** *LMI region*

*A subset $D$ of the complex plane is called an LMI region if there exist a symmetric matrix $L_{reg} = L_{reg}^T \in \mathbb{R}^{n \times n}$ and a matrix $M_{reg} \in \mathbb{R}^{n \times n}$ such that*

$$D = \{z = x + jy \in \mathbb{C} \mid L_{reg} + zM_{reg} + \bar{z}M_{reg}^T < 0\} \tag{2.11}$$

**Example 1.**

The vertical half-plane, disk region and conic sector shown in Figure 2.1 can be written in LMI region as

Vertical half-plane

$$\begin{aligned} D &= \{z = x + jy \in \mathbb{C} \mid x < -\alpha\} \\ &= \left\{z = x + jy \in \mathbb{C} \mid \frac{z + \bar{z}}{2} < -\alpha\right\} \\ &= \{z = x + jy \in \mathbb{C} \mid 2\alpha + z + \bar{z} < 0\} \end{aligned}$$

Disk region

$$\begin{aligned} D &= \{z = x + jy \in \mathbb{C} \mid |z|^2 < r^2\} \\ &= \{z = x + jy \in \mathbb{C} \mid -r + \bar{z}r^{-1}z < 0\} \\ &= \left\{z = x + jy \in \mathbb{C} \mid \begin{bmatrix} -r & 0 \\ 0 & -r \end{bmatrix} + z\begin{bmatrix} 0 & 1 \\ 0 & 0 \end{bmatrix} + \bar{z}\begin{bmatrix} 0 & 0 \\ 1 & 0 \end{bmatrix} < 0\right\} \end{aligned}$$

Conic sector

$$
\begin{aligned}
D &= \{z = x + jy \in \mathbb{C} \mid x \tan\theta < -|y|\} \\
&= \{z = x + jy \in \mathbb{C} \mid x\sin\theta + \frac{y^2\cos^2\theta}{x\sin\theta} < 0\} \\
&= \{z = x + jy \in \mathbb{C} \mid \begin{bmatrix} x\sin\theta & y\cos\theta \\ -y\cos\theta & x\sin\theta \end{bmatrix} < 0\} \\
&= \left\{z = x + jy \in \mathbb{C} \mid z\begin{bmatrix} \sin\theta & \cos\theta \\ -\cos\theta & \sin\theta \end{bmatrix} + \bar{z}\begin{bmatrix} \sin\theta & -\cos\theta \\ \cos\theta & \sin\theta \end{bmatrix} < 0\right\}
\end{aligned}
$$
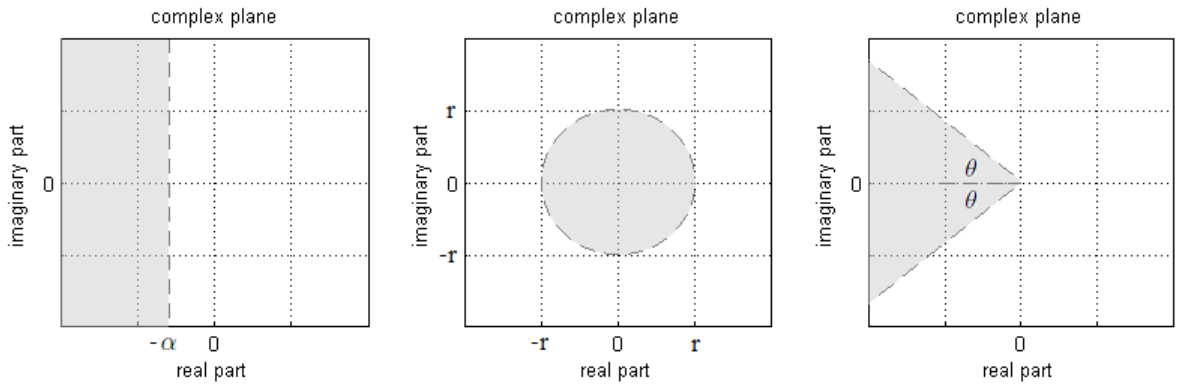


Figure 2.1: LMI region

**Theorem 2.7.** $D$-stability [69]

*The matrix A has all eigenvalues belong to the LMI region* (2.11) *if and only if there exists a symmetric matrix P such that*

$$
L_{reg} \otimes P + M_{reg} \otimes A^T P + M_{reg}^T \otimes PA < 0 \tag{2.12}
$$

*Proof.* Let $\lambda$ be any eigenvalue of A and $v^H, v \in \mathbb{C}^n$ be the left and right eigenvector corresponding to $\lambda$. From the identity:

$$
(I \otimes v^H)(L_{reg} \otimes P + M_{reg} \otimes A^T P + M_{reg}^T \otimes PA)(I \otimes v) = (v^H Pv)(L_{reg} + \lambda M_{reg} + \bar{\lambda} M_{reg}^T)
$$

It's obviously see that the LMI condition in this theorem with $P > 0$ imply $\lambda \in D$ ☐

Applying theorem 2.7, we can design a controller from the following theorem

**Theorem 2.8.** $D$-stabilization [69], [70]

*Consider the system* $\dot{x} = Ax + Bu$ *and a LMI region defined by* (2.11). *If there exist a symmetric matrix* $Y = Y^T > 0$ *and a matrix W satisfying*

$$
L_{reg} \otimes Y + M_{reg} \otimes (AY - BW)^T + M_{reg}^T \otimes (AY - BW) < 0 \tag{2.13}
$$

*Then, the state feedback controller* $u = WY^{-1}x$ *yields the closed-loop system with all eigenvalues in the LMI region.*

*Proof.* The derivation is done in a similar fashion to the theorem 2.5 by multiplying both left and right the equation (2.12) by $I \otimes P^{-1}$ instead. $\qquad\qquad\qquad\qquad\qquad\qquad\square$

The limitation of $D$-stabilization is the assignment LMI regions must be a connected set. The complement of this method can be found in [71] which allows the non-connected assignment regions via the partial pole assignment in LMI problem.

Relying on the notion of dominant poles, we can extrapolate the ideas associated with the second order system to higher order system or nonlinear system. Let us review the relationship between pole locations and time-domain performance of the second order system briefly.

Given the transfer function of the second order system is $G(s) = \dfrac{\omega_n^2}{s^2 + 2\zeta\omega_n s + \omega_n^2}$ which has the poles located at

$$ s = -\zeta\omega_n \pm \omega_n \sqrt{\zeta^2 - 1} $$

where $\zeta$ is damping ratio, $\omega_n$ is undamped frequency. The stable system ($\zeta > 0$ or $\alpha > 0$ ) can be classified into three types depend on $\zeta$ as follow

- If $\zeta > 1$ ($\theta = 0, r > \alpha$), the system is overdamped

- If $\zeta = 1$ ($\theta = 0, r = \alpha$), the system is critically damped

- If $0 < \zeta < 1$ ($\theta > 0, r > \alpha$), the system is underdamped and has the complex conjugate poles

$$ s = -\zeta\omega_n \pm j\omega_n\sqrt{1 - \zeta^2} = -\alpha \pm jr\sin\theta \qquad (\alpha = \zeta\omega_n,\ r = \omega_n,\ \zeta = \cos\theta) $$

The important transient performance characteristics for underdamped system are

| | | | | |
|---|---|---|---|---|
| Settling time (2%) | $T_s$ | $=$ | $\dfrac{4}{\zeta\omega_n}$ | $= \dfrac{4}{\alpha}$ |
| Rise time (10% to 90%) | $T_r$ | $=$ | $\dfrac{1 - 0.417\zeta + 2.917\zeta^2}{\omega_n}$ | $= \dfrac{1 - 0.417\cos\theta + 2.917\cos^2\theta}{r}$ |
| Peak time | $T_p$ | $=$ | $\dfrac{\pi}{\omega_n\sqrt{1 - \zeta^2}}$ | $= \dfrac{\pi}{r\sin\theta}$ |
| Damping period | $T_d$ | $=$ | $\dfrac{2\pi}{\omega_n\sqrt{1 - \zeta^2}}$ | $= \dfrac{2\pi}{r\sin\theta}$ |
| Percentage overshoot | $M$ | $=$ | $\exp\left(\dfrac{-\pi\zeta}{\sqrt{1 - \zeta^2}}\right)$ | $= \exp(-\pi\cot\theta)$ |

Note that the effect of increasing $\zeta$ or decreasing $\theta$ tends to decrease the maximum overshoot and the effect of increasing $\omega_n$ or $r$ or $\alpha$ tends to make the system faster ( $\omega_n$ is a scaling factor of time axis)
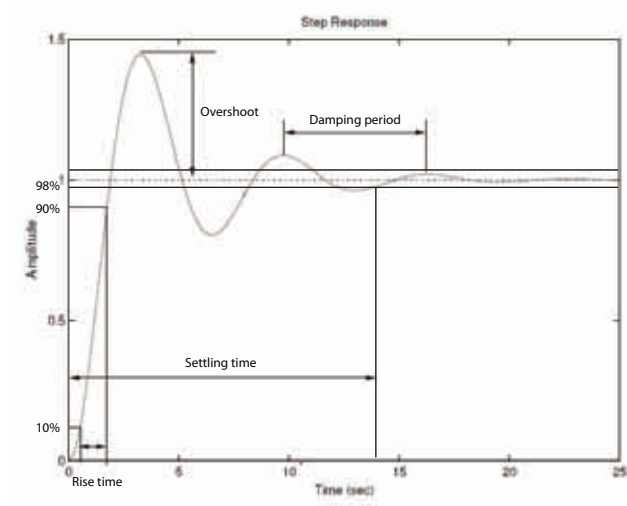
Figure 2.2: Unit step response of the second order system

### 2.3.3   Linear quadratic regulator (LQR)

Assume a continuous-time linear system is

$$\dot{x}(t) = Ax(t) + Bu(t)$$

To design a controller $u = -Lx$ which minimize the cost function:

$$J = \int_0^\infty (x^T(t)Qx(t) + u^T(t)Ru(t))dt \tag{2.14}$$

where $R > 0, Q = H^T H \geq 0$. ( $H$ is obtained from cholesky factorization)

From the Lyapunov stability (Theorem 2.3) with additional positive definite terms, the system is also stable if there exists the Lyapunov function $V(x) > 0$ which satisfy

$$\dot{V}(x) + x^T Q x + u^T R u \quad < \quad 0 \tag{2.15}$$

Assume the system is stable, i.e. $V(x)\big|_{t=\infty} = 0$. The relation between the above condition and the cost function can be shown as follow.

$$\int_0^\infty \dot{V}(x)dt + \int_0^\infty (x^T Q x + u^T R u)dt \quad < \quad 0$$
$$J = \int_0^\infty (x^T Q x + u^T R u)dt \quad < \quad V(x_0) \tag{2.16}$$

Using the above result, we can design the LQR controller gain from the next theorem.

**Theorem 2.9.** LQR controller synthesis  *[70]*

*Consider the system $\dot{x} = Ax + Bu$. The state feedback controller $u = -Lx$ which minimizes the cost function (2.15) can be obtained by solving a symmetric matrix $Y = Y^T > 0$ and a matrix W of the optimization problem:*

$$\max_{Y,W} \quad \text{Tr}(Y)$$

$$\textit{subject to} \quad \begin{bmatrix} YA^T + AY - W^TB^T - BW & YH^T & W^T \\ HY & -I & 0 \\ W & 0 & -R^{-1} \end{bmatrix} < 0 \tag{2.17}$$

*Then, the state feedback controller is* $u = -WY^{-1}x$

*Proof.* Substitute the quadratic Lyapunov function into (2.15). We get

$$(A - BL)^T P + P(A - BL) + Q + L^T RL < 0 \tag{2.18}$$

Multiply both left and right with $P^{-1}$ and introduce the new variables $Y = P^{-1}, W = LY$.

$$YA^T + AY - (LY)^T B^T - BLY + \begin{bmatrix} YH^T & YL^T \end{bmatrix} \begin{bmatrix} I & 0 \\ 0 & R \end{bmatrix} \begin{bmatrix} HY \\ LY \end{bmatrix} < 0 \tag{2.19}$$

By using Schur complement theorem, we get the constraint in this theorem. In order to minimize the cost function (2.15) for all initial value $x_0$, we will minimize $\text{Tr}(Y^{-1})$ or maximize $\text{Tr}(Y)$ where

$$J \quad < \quad V(x_0) \;=\; x_0^T Y^{-1} x_0 \tag{2.20}$$

Finally, we obtain the optimization problem in this theorem. $\qquad\square$

The LMI formulation for LQR controller synthesis may have various forms but some of them lead to the numerical problem in LMI solver. We use the formulation in theorem (2.9) since it works well in practice.

### 2.3.4 Discrete-time controller redesign

Suppose we have designed the continuous-time controller which ensures the desired performance of the closed-loop system. The approximated discrete-time controller can be obtained from the controller redesign technique as follow:

Given a continuous-time system and the corresponding discrete-time system with sampling period $T$

$$\text{continuous}: \quad \dot{x}(t) \quad = \quad Ax(t) + Bu(t)$$
$$\text{discrete}: \quad x[k+1] \quad = \quad A_d x[k] + B_d u[k]$$

where $\quad A_d = e^{AT}, \quad B_d = \int_0^T e^{A\tau} B \, d\tau$

With the designed continuous-time controller $u(t) = -Lx(t)$, the continuous-time closed-loop system and corresponding discrete-time closed-loop system become

$$\text{continuous}: \quad \dot{x}(t) \quad = \quad (A - BL)x(t)$$
$$\text{discrete}: \quad x[k+1] \quad = \quad G_c x[k]$$

where $\quad G_c \quad = \quad e^{(A-BL)T}$

We can find the discrete-time controller $u[k] = -L_d x[k]$ from the following theorem.

**Theorem 2.10** (Controller redesign). *[72]*

*Given the system $\dot{x} = Ax + Bu$ and the continuous-time controller $u(t) = -Lx(t)$. If there exist a symmetric matrix $Y_d = Y_d^T > 0$, a matrix $W$ and a positive scalar $\gamma > 0$ to the optimization problem*

$$\min_{Y_d, W_d} \gamma$$

$$\text{subject to} \quad \begin{bmatrix} -Y_d & (A_d Y_d - B_d W_d)^T \\ (A_d Y_d - B_d W_d) & -Y_d \end{bmatrix} < 0 \tag{2.21}$$

$$\begin{bmatrix} -Y_d & (G_c Y_d - A_d Y_d + B_d W_d)^T \\ (G_c Y_d - A_d Y_d + B_d W_d) & -\gamma I \end{bmatrix} < 0$$

*then the discrete-time controller $u[k] = -W_d Y_d^{-1} x[k]$ can guarantee the stability of this system while give the response of digitally controlled system close to the response of the system controlled by the continuous-time controller.*

*Proof.* Substitute the quadratic Lyapunov function into theorem 2.3 in discrete version. We get

$$V[k+1] - V[k] = x^T[k]((A_d - B_d L_d)^T P_d (A_d - B_d L_d) - P_d)x[k] < 0$$

By using schur complement, the matrix inequality becomes

$$\begin{bmatrix} -P_d & (A_d - B_d L_d)^T \\ (A_d - B_d L_d) & -P_d \end{bmatrix} < 0$$

Multiply both left and right with $\begin{bmatrix} P_d^{-1} & 0 \\ 0 & I \end{bmatrix}$ and introduce the new variables $Y_d = P_d^{-1}$ and $W_d = L_d Y_d$. We get the first LMI condition. Next, the second LMI is used to minimize the difference between discrete-time closed-loop system with discrete-time controller and continuous-time controller by minimize $\gamma$ of the condition:

$$(G_c - (A_d - B_d L_d))^T (G_c - (A_d - B_d L_d)) < \gamma P_d$$

By using the same procedure, we found that the second LMI is equivalent to

$$\begin{bmatrix} P_d^{-1} & 0 \\ 0 & I \end{bmatrix}^T \begin{bmatrix} -P_d & (G_c - A_d + B_d L_d)^T \\ (G_c - A_d + B_d L_d) & -\gamma I \end{bmatrix} \begin{bmatrix} P_d^{-1} & 0 \\ 0 & I \end{bmatrix} < 0$$

$\square$

# CHAPTER III

# BICYCLE SYSTEM MODEL

## 3.1 Bicycle model for both steering and gyroscopic stabilization

### 3.1.1 Model derivation



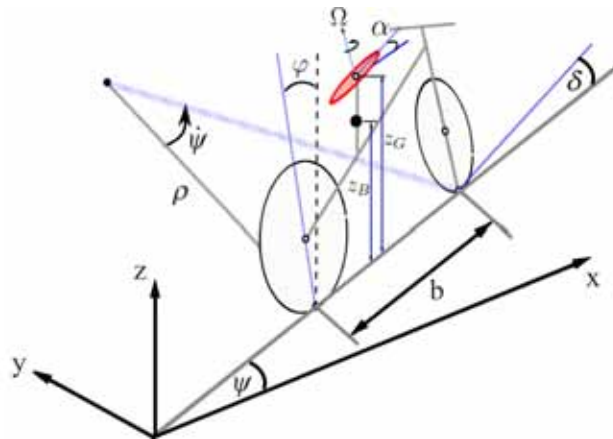Figure 3.1: The bicycle geometry

The provided bicycle geometry, Figure 3.1, contains the physical parameters :

| | |
|---|---|
| $\varphi$ | is the bicycle rolling angle (rad) |
| $\alpha$ | is the flywheel precessing angle (rad) |
| $\delta$ | is the bicycle steering angle (rad) |
| $F_d$ | is the disturbance force (N) |
| $(m_B, m_G)$ | is the mass of bicycle body, gyroscopic flywheel (kg) |
| $(z_B, z_G)$ | is the height of center of mass of bicycle body, gyroscopic flywheel (m) |
| $(I_{Bxx}, I_{Byy}, I_{Bzz})$ | is the bicycle moment of inertia about x, y and z axis (kg-m$^2$) |
| $(I_{Gxx}, I_{Gyy}, I_{Gzz})$ | is the flywheel moment of inertia about x, y and z axis (kg-m$^2$) |
| $\dot{\psi}$ | is the bicycle rotation rate around vertical axis or yaw rate (rad/s) |
| $\sigma$ | is the bicycle forward velocity (m/s) |
| $\Omega$ | is the gyroscopic flywheel spinning angular velocity (rad/s) |
| $b$ | is the bicycle wheel base length (m) |
| $\rho$ | is the track radius curvature (m) |
| $g$ | is the gravitational acceleration (m/s$^2$) |

We follow the derivation of a bicycle model for gyroscopic stabilization in [66] which simplifies the model in [3]. We use this model because it can describe the bicycle dynamic even though the bicycle is moving forward. To keep it simple, we assume that

- The steering axis has no trail and is perpendicular to the ground.

- The steering angle $\delta$ is the control variable. So the rotational degree of freedom associated with the front fork then disappears. Moreover, the steering angular velocity is assumed to be small.

- The bicycle moves on a flat plane.

- The tires have no width and no deformation.

- The bicycle rolls without slipping that implies the yaw rate $\dot{\psi} = \dfrac{\sigma}{\rho} \approx \dfrac{\sigma \tan \delta}{b}$ (see Figure 3.2)

- The moment of inertia of the front and rear wheel are neglected.

- All inertia products, i.e. $I_{Bxy}, I_{Bxz}, I_{Byz}, I_{Gxy}, I_{Gxz}$ and $I_{Gyz}$, are also neglect.
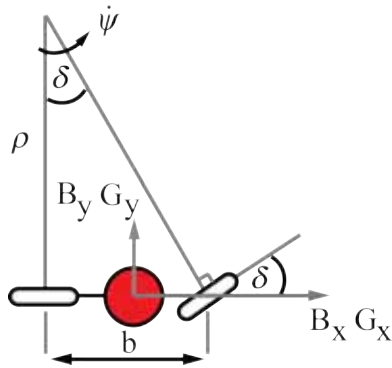


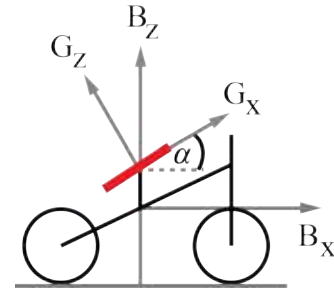Figure 3.2: Top view of the bicycle



Figure 3.3: Side view of the bicycle

The model derivation is done by Lagrangian method. The bicycle will be separated into 2 parts including body and gyroscopic flywheel. The total kinetic energy T of the system is

$$T = \frac{1}{2} m_B \mathbf{v_B}^T \mathbf{v_B} + \frac{1}{2} \boldsymbol{\omega_B}^T \mathbf{I_B} \boldsymbol{\omega_B} + \frac{1}{2} m_G \mathbf{v_G}^T \mathbf{v_G} + \frac{1}{2} \boldsymbol{\omega_G}^T \mathbf{I_G} \boldsymbol{\omega_G} \tag{3.1}$$

where

$$\mathbf{v_B} = \dot{\psi} \begin{bmatrix} z_B \sin \varphi \\ 0 \\ 0 \end{bmatrix} + \dot{\varphi} \begin{bmatrix} 0 \\ z_B \\ 0 \end{bmatrix} + \begin{bmatrix} \sigma \\ 0 \\ 0 \end{bmatrix} \qquad \boldsymbol{\omega_B} = \dot{\psi} \begin{bmatrix} 0 \\ \sin \varphi \\ \cos \varphi \end{bmatrix} + \dot{\varphi} \begin{bmatrix} 1 \\ 0 \\ 0 \end{bmatrix}$$

$$\mathbf{v_G} = \dot{\psi} \begin{bmatrix} z_G \sin \varphi \\ 0 \\ 0 \end{bmatrix} + \dot{\varphi} \begin{bmatrix} 0 \\ z_G \\ 0 \end{bmatrix} + \begin{bmatrix} \sigma \\ 0 \\ 0 \end{bmatrix} \qquad \boldsymbol{\omega_G} = \dot{\psi} \begin{bmatrix} -\cos \varphi \sin \alpha \\ \sin \varphi \\ \cos \varphi \cos \alpha \end{bmatrix} + \dot{\varphi} \begin{bmatrix} \cos \alpha \\ 0 \\ \sin \alpha \end{bmatrix} + \begin{bmatrix} 0 \\ \dot{\alpha} \\ \Omega \end{bmatrix}$$

Also the potential energy V of the system is

$$V = m_B z_B g \sin \varphi + m_G z_G g \sin \varphi \tag{3.2}$$

We define the generalized coordinates as

$$q_1 = \varphi \qquad : \quad \text{Bicycle rolling angle}$$

$$q_2 = \alpha \qquad : \quad \text{Flywheel precession angle}$$

Hence, the generalized forces are

$$Q_1 = F_d z_B \cos \varphi \quad : \quad \text{Torque due to lateral disturbance force}$$

$$Q_2 = \tau_\alpha \qquad : \quad \text{Torque due to the precessing motor}$$

Formulate the Lagrange's equations as follows:

$$\frac{d}{dt}\left(\frac{\partial T}{\partial \dot{q}_k}\right) - \frac{\partial T}{\partial q_k} + \frac{\partial V}{\partial q_k} = Q_k \tag{3.3}$$

Substitute each term in equation (3.3) and rearrange the equations. We get the equations of motion:

*Bicycle rolling equation*

$$
\left.
\begin{aligned}
&(k_2 + k_3 + k_6 \sin^2 \alpha)\ddot{\varphi} + k_6 \dot{\varphi}\dot{\alpha} \sin 2\alpha - k_1 \sigma \dot{\psi} \cos \varphi \\
&+ \dot{\psi}\dot{\alpha}(k_6 \cos 2\alpha - I_{Gyy}) \cos \varphi - 0.5\dot{\psi}^2(k_7 - k_6 \cos^2 \alpha) \sin 2\varphi \\
&+ I_{Gzz}\Omega(\dot{\alpha} + \dot{\psi} \sin \varphi) \cos \alpha - k_1 g \sin \varphi
\end{aligned}
\right\} = F_d z_T \cos \varphi \tag{3.4}
$$

*Gyroscopic flywheel precessing equation*

$$
\left.
\begin{aligned}
&I_{Gyy}\ddot{\alpha} + \dot{\psi}\dot{\varphi}(I_{Gyy} - k_6 \cos 2\alpha) \cos \varphi + 0.5 k_6(\dot{\psi}^2 \cos^2 \varphi - \dot{\varphi}^2) \sin 2\alpha \\
&+ I_{Gzz}\Omega(\dot{\psi} \cos \varphi \sin \alpha - \dot{\varphi} \cos \alpha)
\end{aligned}
\right\} = \tau_\alpha
$$

$$\tag{3.5}$$

where

$$k_1 = m_B z_B + m_G z_G \qquad\qquad k_2 = m_B z_B^2 + m_G z_G^2$$

$$k_3 = I_{Bxx} + I_{Gxx} \qquad\qquad k_4 = I_{Byy} + I_{Gyy}$$

$$k_5 = I_{Bzz} + I_{Gzz} \qquad\qquad k_6 = I_{Gzz} - I_{Gxx}$$

$$k_7 = k_4 - I_{Bzz} - I_{Gxx}$$

### 3.1.2 Model analysis

We have neglect the front fork steering dynamic under the assumption that our steering motor can track the desired steering angle fast enough and the desired steering angle is changed slowly. Most authors use only the gyroscopic effect to stabilize the bicycle. But we will take the advantage of the centrifugal force in this model to stabilize the bicycle too. The interpretation of each term in

Table 3.1: Torque definition

| Dynamic term | Symbol | Torque description |
|---|---|---|
| *Bicycle rolling equation* | | |
| $-k_6\dot{\varphi}\dot{\alpha}\sin 2\alpha$ | $\tau_{B\dot{\varphi}\dot{\alpha}}$ | Torque depend on bicycle rolling and flywheel precession |
| $k_1\sigma\dot{\psi}\cos\varphi$ | $\tau_{B\dot{\psi}}$ | Torque due to centrifugal force |
| $-\dot{\psi}\dot{\alpha}(k_6\cos 2\alpha - I_{Gyy})\cos\varphi$ | $\tau_{B\dot{\psi}\dot{\alpha}}$ | Torque depend on bicycle yawing and flywheel precession |
| $0.5\dot{\psi}^2(k_7 - k_6\cos^2\alpha)\sin 2\varphi$ | $\tau_{B\dot{\psi}^2}$ | Torque depend on the square of yaw rate on bicycle |
| $-I_{Gzz}\Omega\dot{\alpha}\cos\alpha$ | $\tau_{B\Omega\dot{\alpha}}$ | Gyroscopic torque of flywheel precession turn spin axis |
| $-I_{Gzz}\Omega\dot{\psi}\sin\varphi\cos\alpha$ | $\tau_{B\Omega\dot{\psi}}$ | Gyroscopic torque of bicycle yawing turn spin axis |
| $k_1 g\sin\varphi$ | $\tau_{Bg}$ | Torque due to gravity force |
| *Gyroscopic flywheel precessing equation* | | |
| $\dot{\psi}\dot{\varphi}(k_6\cos 2\alpha - I_{Gyy})\cos\varphi$ | $\tau_{G\dot{\psi}\dot{\varphi}}$ | Torque depend on yaw rate and bicycle rolling |
| $-0.5k_6\dot{\psi}^2\cos^2\varphi\sin 2\alpha$ | $\tau_{G\dot{\psi}^2}$ | Torque depend on the square of yaw rate on flywheel |
| $0.5k_6\dot{\varphi}^2\sin 2\alpha$ | $\tau_{G\dot{\varphi}^2}$ | Torque depend on the square of rolling rate |
| $-I_{Gzz}\Omega\dot{\psi}\cos\varphi\sin\alpha$ | $\tau_{G\Omega\psi}$ | Gyroscopic torque of bicycle yawing turn spin axis |
| $I_{Gzz}\Omega\dot{\varphi}\cos\alpha$ | $\tau_{G\Omega\dot{\varphi}}$ | Gyroscopic torque of bicycle rolling turn spin axis |
| $K_{t,m2}I_{m2} - B_{eq,m2}\dot{\alpha}$ | $\tau_\alpha$ | Torque due to precessing motor |

the equations of motion has been shown in Table 3.1. The bicycle model for gyroscopic stabilization contain a lot of coupling effect between each state variables, i.e. $\varphi, \dot{\varphi}, \alpha$ and $\dot{\alpha}$. Using the bicycle parameters given in Table A.1 and control law proposed in [67] with forward velocity $\sigma = 2$ m/s, yaw rate $\dot{\psi} = 0.3$ rad/s and initial condition $\mathbf{x}_0 = \begin{bmatrix} 0.05 & 0 & 0 & 0 \end{bmatrix}^T$. The simulation results show all torque components acting on the bicycle and flywheel in Figure 3.4. The major effects for bicycle stabilization are $\tau_{B\Omega\dot{\alpha}}$ and $\tau_{B\dot{\psi}}$ like a basic principle for gyroscopic stabilization and steering stabilization respectively.

$\tau_{B\Omega\dot{\alpha}}$ is a torque due to gyroscopic effect from the precessing of flywheel. It is proportional to a flywheel spinning velocity ($\Omega$) and a flywheel precessing angular velocity ($\dot{\alpha}$). For the best performance, we should operate the flywheel around zero precessing angle because its effect will be reduced with a factor of $\cos\alpha$. This torque plays an important role in bicycle stabilization under low forward speed.

$\tau_{B\dot{\psi}}$ is a torque due to centrifugal force which is proportional to a square of forward speed ($\sigma^2$) and is also approximately proportional to a steering angle ($\delta$). When the bicycle is moving with sufficient high speed, this effect will dominate the gyroscopic effect and become the main stabilizer.
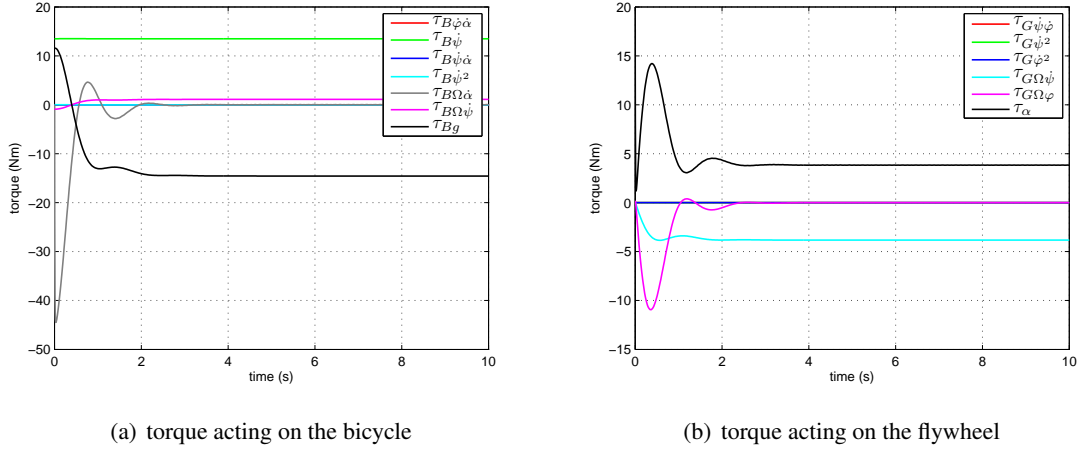
(a) torque acting on the bicycle        (b) torque acting on the flywheel

Figure 3.4: Comparison of torque components in the bicycle model

In this thesis, we define the state variables as $\mathbf{x} = \begin{bmatrix} \varphi & \alpha & \dot{\varphi} & \dot{\alpha} \end{bmatrix}^T$ and input $\mathbf{u} = \begin{bmatrix} \dot{\psi}(\delta) & \tau_\alpha \end{bmatrix}^T$. Consider the equilibrium points of this model by setting the derivative of the state $\dot{\mathbf{x}} = 0$, disturbance force $F_d = 0$ and torque of precessing motor $\tau_\alpha = 0$. The system model becomes

*Bicycle rolling equation*

$$-k_1\sigma\dot{\psi}\cos\varphi - 0.5\dot{\psi}^2(k_7 - k_6\cos^2\alpha)\sin 2\varphi + I_{Gzz}\Omega\dot{\psi}\sin\varphi\cos\alpha - k_1 g\sin\varphi = 0 \quad (3.6)$$

*Gyroscopic flywheel precessing equation*

$$0.5k_6\dot{\psi}^2\cos^2\varphi\sin 2\alpha + I_{Gzz}\Omega\dot{\psi}\cos\varphi\sin\alpha \quad = \quad 0 \quad (3.7)$$

From the gyroscopic flywheel precessing equation implies $\dot{\psi} = 0$ or $\sin\alpha = 0$ or $\cos\varphi = 0$ or $k_6\dot{\psi}\cos\varphi\cos\alpha = -I_{Gzz}\Omega$

- When $\dot{\psi} = 0$ ($\delta = 0$ or $\sigma = 0$)

   Bicycle rolling equation       $k_1 g\sin\varphi \quad = \quad 0$

   The equilibrium points are $(\varphi, \alpha, \dot{\psi}) = (0, \alpha_e, 0)$  ;   $\alpha_0 \in R$

   If $\sigma = 0$, the equilibrium points are $(\varphi, \alpha, \delta) = (0, \alpha_e, \delta_e)$  ;   $\alpha_e \in R, \delta_e \in R$

   If $\sigma \neq 0$, the equilibrium points are $(\varphi, \alpha, \delta) = (0, \alpha_e, 0)$  ;   $\alpha_e \in R$

- When $\cos\varphi = 0$ ($\varphi = \pm\dfrac{\pi}{2}$)

   Bicycle rolling equation       $I_{Gzz}\Omega\dot{\psi}\cos\alpha - k_1 g \quad = \quad 0$

   Assume $\dot{\psi} = \dot{\psi}_e$ is an equilibrium point

   The equilibrium points are $(\varphi, \alpha, \dot{\psi}) = (0, \arccos\left(\dfrac{k_1 g}{I_{Gzz}\Omega\dot{\psi}_e}\right), \dot{\psi}_e)$  ;   $\dot{\psi}_e \in R$

   However, it's impossible to operate under this condition

- When $\sin \alpha = 0$ $(\alpha = 0)$

  Bicycle rolling equation
  $$-k_1 \dot{\psi} \sigma \cos \varphi - 0.5 \dot{\psi}^2 (k_7 - k_6) \sin 2\varphi$$
  $$+ I_{Gzz} \Omega \dot{\psi} \sin \varphi - k_1 g \sin \varphi \quad = \quad 0$$

  Assume $\dot{\psi} = \dot{\psi}_e$ is an equilibrium point

  If $\varphi = 0$, the equilibrium point is $(\varphi, \alpha, \dot{\psi}) = (\varphi, \alpha, \delta) = (0, 0, 0)$

  If $\varphi \neq 0$, the equilibrium points are $(\varphi, \alpha, \delta) = (\varphi_e(\delta_e), 0, \delta_e)$ which satisfy above equation. The equilibrium points of this case are shown in Figure 3.5. And it should be noted that the effects of turning left and right are not symmetry for a single gyroscopic flywheel
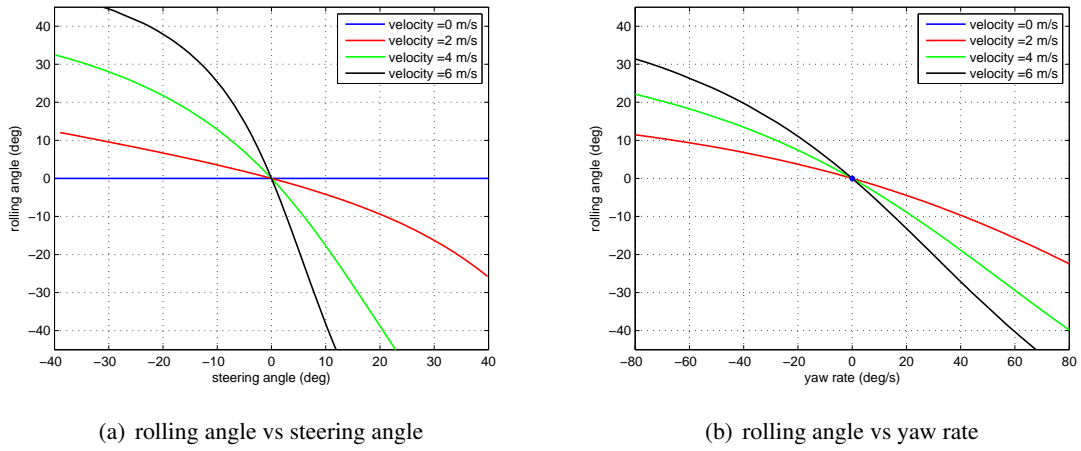


(a) rolling angle vs steering angle
(b) rolling angle vs yaw rate

Figure 3.5: Equilibrium point at zero precessing angle

- When $k_6 \dot{\psi} \cos \varphi \cos \alpha = -I_{Gzz} \Omega$

  Bicycle rolling equation
  $$-k_1 \sigma \dot{\psi} \cos \varphi - 0.5 \dot{\psi}^2 (k_7 - k_6 \cos^2 \alpha) \sin 2\varphi$$
  $$+ I_{Gzz} \Omega \dot{\psi} \sin \varphi \cos \alpha - k_1 g \sin \varphi \quad = \quad 0$$

  It's too complicated for finding the equilibrium points in explicit form

### 3.1.3 Linearized model

We examine the stability of the equilibrium points via linearization technique. Moreover, we will design the controller from this model to compare with our designed controller in the next section. Let define the deviation variables to measure the difference.

$$\Delta \mathbf{x} \triangleq \mathbf{x} - \mathbf{x_e}, \qquad \Delta \mathbf{u} \triangleq \mathbf{u} - \mathbf{u_e}$$

Then, we linearize the nonlinear model (3.4) and (3.5) about the equilibrium point $\mathbf{x}_e = \begin{bmatrix} \varphi_e & 0 & 0 & 0 \end{bmatrix}^T$ with equilibrium input $\mathbf{u}_e = \begin{bmatrix} \dot{\psi}_e & 0 \end{bmatrix}^T$. We get

$$(k_2 + k_3)\ddot{\varphi} + k_1\sigma(\dot{\psi}_e \sin\varphi_e \Delta\varphi - \cos\varphi_e \Delta\dot{\psi})$$
$$-(k7 - k6)(\dot{\psi}_e \sin 2\varphi_e \Delta\dot{\psi} + \dot{\psi}_e^2 \cos 2\varphi_e \Delta\varphi)$$
$$+I_{Gzz}\Omega(\Delta\dot{\alpha} + \sin\varphi_e \Delta\dot{\psi} + \dot{\psi}_e \cos\varphi_e \Delta\varphi) \qquad (3.8)$$
$$+\dot{\psi}_e(k_6 - I_{Gyy})\cos\varphi_e \Delta\dot{\alpha} - k_1 g\Delta\varphi \qquad = \qquad 0$$

$$I_{Gyy}\ddot{\alpha} + \dot{\psi}_e(I_{Gyy} - k_6)\cos\varphi_e \Delta\dot{\varphi}$$
$$+k_6\dot{\psi}_e^2 \cos^2\varphi_e \Delta\alpha + I_{Gzz}\Omega(\dot{\psi}\Delta\alpha - \Delta\dot{\varphi}) \qquad = \qquad \Delta\tau_\alpha \qquad (3.9)$$

Rearrange into a state-space representation :

$$\frac{d}{dt}\begin{bmatrix} \varphi \\ \alpha \\ \dot{\varphi} \\ \dot{\alpha} \end{bmatrix} = \begin{bmatrix} 0 & 0 & 1 & 0 \\ 0 & 0 & 0 & 1 \\ a_{31} & 0 & 0 & a_{34} \\ 0 & a_{42} & a_{43} & 0 \end{bmatrix}\begin{bmatrix} \Delta\varphi \\ \Delta\alpha \\ \Delta\dot{\varphi} \\ \Delta\dot{\alpha} \end{bmatrix} + \begin{bmatrix} 0 & 0 \\ 0 & 0 \\ b_{31} & 0 \\ 0 & b_{42} \end{bmatrix}\begin{bmatrix} \Delta\dot{\psi} \\ \Delta\tau_\alpha \end{bmatrix} \qquad (3.10)$$

where

$$a_{31} = \frac{-k_1\sigma\dot{\psi}_e \sin\varphi_e + \dot{\psi}_e^2(k_7 - k_6)\cos 2\varphi_e - I_{Gzz}\Omega\dot{\psi}_e \cos\varphi_e + k_1 g\cos\varphi_e}{k_2 + k_3}$$

$$a_{34} = \frac{-\dot{\psi}_e(k_6 - I_{Gyy})\cos\varphi_e - I_{Gzz}\Omega}{k_2 + k_3}$$

$$b_{31} = \frac{k_1\sigma\cos\varphi_e + \dot{\psi}_e(k_7 - k_6)\sin 2\varphi_e - I_{Gzz}\Omega\sin\varphi_e}{k_2 + k_3}$$

$$a_{42} = \frac{-k_6\dot{\psi}_e^2 \cos^2\varphi_e - I_{Gzz}\Omega\dot{\psi}_e \cos\varphi_e}{I_{Gyy}}$$

$$a_{43} = \frac{-\dot{\psi}_e(I_{Gyy} - k_6)\cos\varphi_e + I_{Gzz}\Omega}{I_{Gyy}}$$

$$b_{42} = \frac{1}{I_{Gyy}}$$

Note that when the equilibrium point is $\mathbf{x}_e = \begin{bmatrix} 0 & 0 & 0 & 0 \end{bmatrix}^T$, $\mathbf{u}_e = \begin{bmatrix} 0 & 0 \end{bmatrix}^T$. The linearized model parameter will be simplified into

$$a_{31} = \frac{k_1 g\cos\varphi_e}{k_2 + k_3} \quad, a_{34} = \frac{-I_{Gzz}\Omega}{k_2 + k_3} \quad, b_{31} = \frac{k_1\sigma}{k_2 + k_3} \quad, a_{42} = 0 \quad, a_{43} = \Omega \quad, b_{42} = \frac{1}{I_{Gyy}}$$

We will focus on the equilibrium point at $\alpha_e = 0$ for the best performance of gyroscopic flywheel actuator. Four eigenvalues of the linearization model around the equilibrium point at -1 rad/s to 1 rad/s yaw rate have been shown in Figure 5.1. They are pure imaginary roots or contain a positive real eigenvalue. So it can imply that most of them are unstable but it cannot conclude the stability for some equilibrium points by linearization technique. Figure 5.2 show the response of rolling angle and precessing angle with different 4 initial conditions for the autonomous system. Although the velocity parameter affects the eigenvalues of the system, the pole trajectory is also moving in the same pattern.
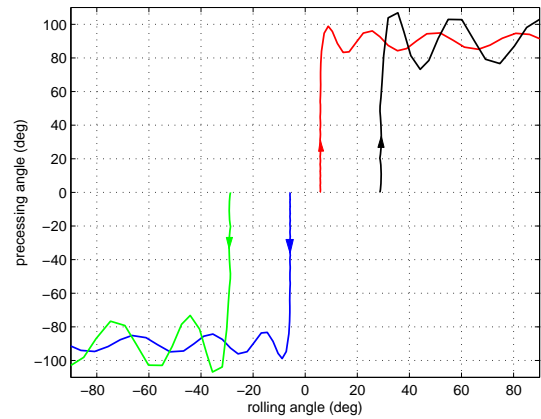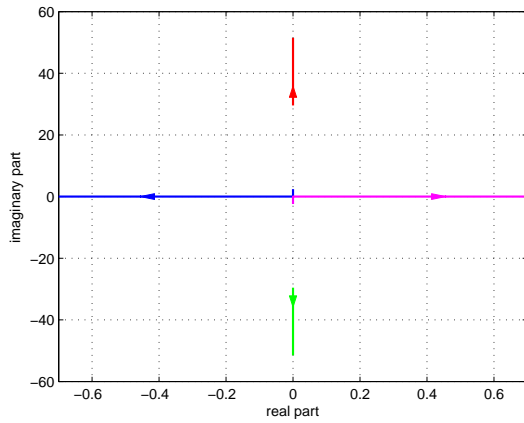
Figure 3.6: Poles trajectory of linearized model with the velocity 1 m/s

Figure 3.7: Phase portrait of open loop responses with 4 initial conditions

### 3.1.4 Piecewise affine model

We divide both bicycle rolling angle $(x_1)$ and flywheel precessing angle $(x_2)$ into 3 regions. So the overall system is divided into 9 regions as shown in Figure 3.8. We approximate the bicycle nonlinear model (3.4)–(3.5) with a PWA model by using least square error with discontinuous boundary method in section 2.2.2 because it is simple and also gives the smallest error compare to another method as shown in [68]. Applying this approximation method over the operating region $x_1 \in [-30, 30]$ degree, $x_2 \in [-30, 30]$ degree, $x_3 \in [-30, 30]$ degree/s and $x_4 \in [-50, 50]$ degree/s with the same parameters in Table A.1, we get the PWA model in state-space form (2.1) as follows.
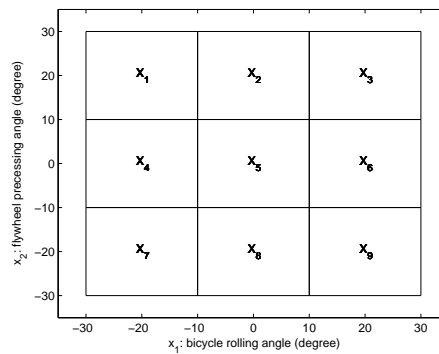


Figure 3.8: Polyhedral partition of the bicycle state.

**Piecewise affine model of the bicycle using both steering and gyroscopic stabilization**

$$A_1 = \begin{bmatrix} 0 & 0 & 1 & 0 \\ 0 & 0 & 0 & 1 \\ 10.230 & -0.019 & 0 & -2.977 \\ -0.054 & 0.007 & 388.496 & -0.011 \end{bmatrix} \quad A_2 = \begin{bmatrix} 0 & 0 & 1 & 0 \\ 0 & 0 & 0 & 1 \\ 10.238 & 0 & 0 & -3.171 \\ -0.006 & 0.006 & 413.739 & -0.003 \end{bmatrix}$$

$$A_3 = \begin{bmatrix} 0 & 0 & 1 & 0 \\ 0 & 0 & 0 & 1 \\ 10.230 & 0.020 & 0 & -2.977 \\ 0.042 & -0.049 & 389.073 & -0.013 \end{bmatrix} \quad A_4 = \begin{bmatrix} 0 & 0 & 1 & 0 \\ 0 & 0 & 0 & 1 \\ 10.886 & 0.002 & 0 & -2.977 \\ 0.090 & 0.073 & 388.447 & 0.002 \end{bmatrix}$$

$$A_5 = \begin{bmatrix} 0 & 0 & 1 & 0 \\ 0 & 0 & 0 & 1 \\ 10.896 & 0 & 0 & -3.171 \\ 0.001 & 0.015 & 413.736 & 0 \end{bmatrix} \quad A_6 = \begin{bmatrix} 0 & 0 & 1 & 0 \\ 0 & 0 & 0 & 1 \\ 10.885 & 0 & 0.001 & -2.977 \\ -0.081 & -0.162 & 389.087 & -0.027 \end{bmatrix}$$

$$A_7 = \begin{bmatrix} 0 & 0 & 1 & 0 \\ 0 & 0 & 0 & 1 \\ 10.231 & 0.016 & 0 & -2.977 \\ 0.040 & 0.045 & 388.498 & -0.005 \end{bmatrix} \quad A_8 = \begin{bmatrix} 0 & 0 & 1 & 0 \\ 0 & 0 & 0 & 1 \\ 10.238 & 0 & 0 & -3.171 \\ 0.005 & -0.007 & 413.73 & -0.002 \end{bmatrix}$$

$$A_9 = \begin{bmatrix} 0 & 0 & 1 & 0 \\ 0 & 0 & 0 & 1 \\ 10.229 & -0.018 & 0 & -2.977 \\ 0.131 & -0.011 & 389.075 & -0.017 \end{bmatrix} \quad B_1 = B_2 = ... = B_9 = \begin{bmatrix} 0 & 0 \\ 0 & 0 \\ 2.228 & 0 \\ 0 & 7.246 \end{bmatrix}$$

$$a_1 = \begin{bmatrix} 0 \\ 0 \\ -0.151 \\ -0.011 \end{bmatrix}, \quad a_2 = \begin{bmatrix} 0 \\ 0 \\ -0.145 \\ -0.003 \end{bmatrix}, \quad a_3 = \begin{bmatrix} 0 \\ 0 \\ -0.152 \\ 0.025 \end{bmatrix}, \quad a_4 = \begin{bmatrix} 0 \\ 0 \\ 0.001 \\ 0.020 \end{bmatrix}, \quad a_5 = \begin{bmatrix} 0 \\ 0 \\ 0 \\ 0 \end{bmatrix}$$

$$a_6 = \begin{bmatrix} 0 \\ 0 \\ 0 \\ 0.045 \end{bmatrix}, \quad a_7 = \begin{bmatrix} 0 \\ 0 \\ 0.150 \\ 0.006 \end{bmatrix}, \quad a_8 = \begin{bmatrix} 0 \\ 0 \\ 0.145 \\ -0.001 \end{bmatrix}, \quad a_9 = \begin{bmatrix} 0 \\ 0 \\ 0.152 \\ -0.047 \end{bmatrix}$$

$$C_1 = C_2 = ... = C_9 = \begin{bmatrix} 1 & 0 \end{bmatrix}$$

$$c_1 = c_2 = ... = c_9 = 0$$
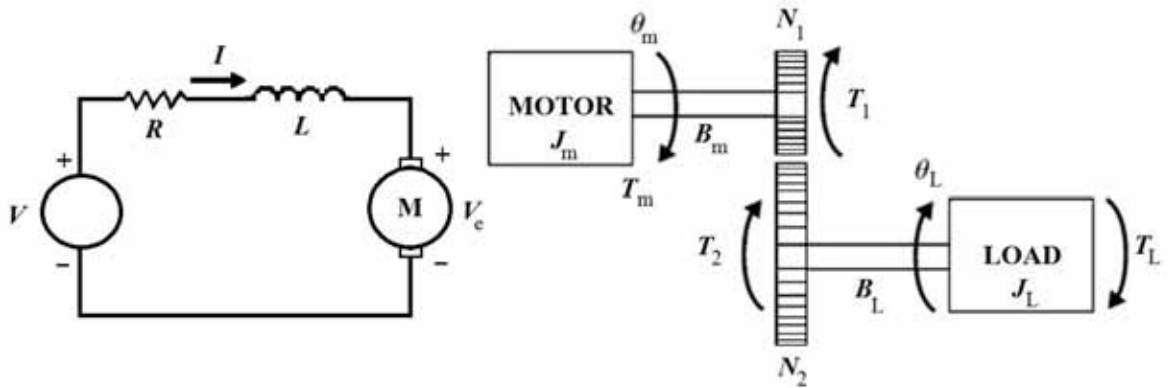
## 3.2 Direct current (DC) motor model



Figure 3.9: DC motor with gear

The mechanical linkages between the motor and the load in a gear drive with an equivalent motor circuit have been shown in Figure 3.9. The related parameters are

$(\theta_m, \theta_L)$    is rotor and load shaft position (rad)

$K_e$    is the electromotive force constant (V-s/rad)

$K_t$    is the torque constant (N-m/A)

$I$    is the armature current (A)

$V$    is the armature voltage (V)

$(N_1, N_2)$    is the number of teeth on a gear of motor and load

$(J_m, J_L)$    is the moment of inertia of motor and load (kg-m$^2$)

$(B_m, B_L)$    is the viscous damping of motor and load (N-m-s/rad)

$R$    is the terminal resistance ($\Omega$)

$L$    is the terminal inductance (H)

We derive a simple linear model of DC motor under the assumptions mentioned below.

- The armature resistance and inductance can be regarded as constant

- The effect of armature reaction and brush voltage drop have been neglected

- The static friction is negligible and the frictional torque is proportional to angular velocity.

From the equivalent circuit diagram, the electrical differential equation obtained from Kirchhoff's voltage law is written as

$$L\frac{dI}{dt} = V - RI - V_e \qquad (3.11)$$

where    back-emf is defined as    $V_e = K_e \frac{d\theta_m}{dt}$

From the mechanical diagram, the equations of motion obtained from Newton's law are written as

At motor:

$$J_m \frac{d^2\theta_m}{dt^2} = T_m - B_m \frac{d\theta_m}{dt} - T_1 \tag{3.12}$$

At load:

$$J_L \frac{d^2\theta_L}{dt^2} = T_2 - B_L \frac{d\theta_L}{dt} - T_L \tag{3.13}$$

where $\quad T_m \;=\; K_t I \quad$ is the torque generated by the motor

And apply the relationship between two ideal gears:

$$\frac{N_1}{N_2} = \frac{T_1}{T_2} = \frac{\theta_L}{\theta_m} = \frac{\dot{\theta}_L}{\dot{\theta}_m} \tag{3.14}$$

Then, the governing equations of DC motor system are

$$L\frac{dI}{dt} = V - RI - NK_e \frac{d\theta_L}{dt} \tag{3.15}$$

$$J_{eq} \frac{d^2\theta_L}{dt^2} = NK_t I - B_{eq} \frac{d\theta_L}{dt} - T_L \tag{3.16}$$

where $\quad N \;=\; \dfrac{N_2}{N_1} \qquad$ is the turns ratio

$\qquad\quad J_{eq} \;=\; J_L + N^2 J_m \quad$ is the equivalent moment of inertia at load shaft

$\qquad\quad B_{eq} \;=\; B_L + N^2 B_m \quad$ is the equivalent viscous damping at load shaft

Using Laplace transforms, we get the transfer function as follows.

when the output is a speed

$$\frac{\dot{\theta}_L(s)}{V(s)} = \frac{K_t}{(J_{eq}s + B_{eq})(Ls + R) + K_e K_t} \tag{3.17}$$

when the output is a position

$$\frac{\theta_L(s)}{V(s)} = \frac{K_t}{s((J_{eq}s + B_{eq})(Ls + R) + K_e K_t)} \tag{3.18}$$

Or rewrite the above dynamic equations in a state-space form

$$\frac{d}{dt}\begin{bmatrix} \theta_L \\ \dot{\theta}_L \\ I \end{bmatrix} = \begin{bmatrix} 0 & 1 & 0 \\ 0 & -\dfrac{B_{eq}}{J_{eq}} & \dfrac{NK_t}{J_{eq}} \\ 0 & -\dfrac{NK_e}{L} & -\dfrac{R}{L} \end{bmatrix} \begin{bmatrix} \theta_L \\ \dot{\theta}_L \\ I \end{bmatrix} + \begin{bmatrix} 0 \\ 0 \\ \dfrac{1}{L} \end{bmatrix} V$$

# CHAPTER IV

# CONTROLLER DESIGN FOR STABILIZATION SYSTEM

## 4.1 State feedback redesign for PWA system with regional pole placement performance

A state feedback gain for stabilizing a bicycle is designed in two steps. We design a continuous-time controller first and then we convert it into a discrete-time controller in the second step.

### 4.1.1 Controller synthesis for PWA system with regional pole placement performance

To design a continuous-time controller, we combine 3 controller design techniques including 1) Regional pole placement, 2) Linear quadratic regulator, 3) Piecewise quadratic stabilization.

Since the regional pole placement, linear quadratic regulator and piecewise quadratic stabilization technique can be formulated in LMIs problem. We will combine these techniques and illustrate the advantage of this method.

Using the regional pole placement technique with the intersection of all LMI regions in example 1, we can design the controller to ensure many requirements of the closed-loop system [See section 2.3.2]. In more detail, we can ensure that the closed-loop system will decay faster than $e^{-\alpha_p t}$, have a minimum damping ratio $\zeta = \cos\theta$ and a maximum damped natural frequency $\omega_0 = r\sin\theta$ around the operating region by the following constraints:

$$A_5 Y + Y A_5^T - B_5 W - W^T B_5^T + 2\alpha_p Y \quad < \quad 0 \quad : \quad \text{Vertical strip}$$

$$\begin{bmatrix} -rY & A_5 Y - B_5 W \\ Y A_5^T - W^T B_5^T & -rY \end{bmatrix} \quad < \quad 0 \quad : \quad \text{Disk}$$

$$\begin{bmatrix} \sin\theta(Y A_5^T - W^T B_5^T + A_5 Y - B_5 W) & \cos\theta(Y A_5^T - W^T B_5^T - A_5 Y + B_5 W) \\ \cos\theta(-Y A_5^T + W^T B_5^T + A_5 Y - B_5 W) & \sin\theta(Y A_5^T - W^T B_5^T + A_5 Y - B_5 W) \end{bmatrix} \quad < \quad 0 \quad : \quad \text{Conic sector}$$

$$(4.1)$$

Combining with the LQR technique, it provides the smallest possible to both control signal and states of the controlled system. We can tune the system to meet a desired performance via the weighting matrices. Typically, the stability margins may be very small (small robustness) but this disadvantage can be recovered by increasing $\alpha_p$ for a vertical half-plane constraint. The LMI
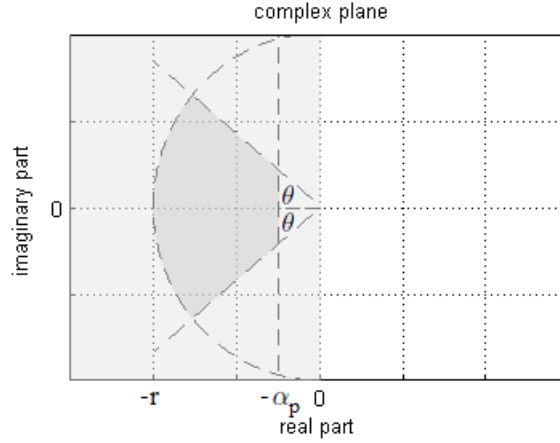
Figure 4.1: Combined LMI region

formulation for LQR technique is

$$
\max_{Y,W} \quad \mathrm{Tr}(Y)
$$

$$
\text{subject to} \quad
\begin{bmatrix}
Y A_5^T + A_5 Y - W^T B_5^T - B_5 W & Y H^T & W^T \\
HY & -I & 0 \\
W & 0 & -R^{-1}
\end{bmatrix} < 0
\tag{4.2}
$$

Moreover, we use the piecewise affine technique to extend the stability region of nonlinear system by giving the additional constraints:

$$
\begin{bmatrix}
Y A_i^T + A_i Y - (B_i W)^T - B_i W - v_i a_i a_i^T & Y S_i^T - v_i a_i s_i^T \\
(Y S_i^T - v_i a_i s_i^T)^T & v_i (I - s_i s_i^T)
\end{bmatrix} < 0 \ \text{ for all } i \neq 5
\tag{4.3}
$$

Note that we apply (2.13), (2.17), (2.21) only on the model which contains the equilibrium point and we neglect the first LMI in (2.10) because this constraint is already included in (2.13)

**Numerical result**

Recall the numerical result in section 3.1.4, the PWA model of the bicycle obtained by approximating the nonlinear of the bicycle (3.4)–(3.5) is written in state space form as

$$
\left.
\begin{aligned}
\dot{x} &= A_i x + a_i + B_i u \\
y &= C_i x + c_i
\end{aligned}
\right\} \quad x \in X_i
\tag{4.4}
$$

where $x = \begin{bmatrix} \varphi & \alpha & \dot{\varphi} & \dot{\alpha} \end{bmatrix}^T$ is the state variable and $u = \begin{bmatrix} \dot{\psi} & \tau_\alpha \end{bmatrix}^T$ is the control input. To stabilize the bicycle to stay upright at $\varphi = 0$, we apply the proposed design method by determining the control specifications of the compensated system for coarse tuning as

(1) settling time less than 4 s $\qquad\qquad\qquad\qquad\qquad$ : $\quad T_s = \dfrac{4}{\alpha_p} < 4$

(2) maximum overshoot less than 0.0008% of the final value $\quad$ : $\quad M = e^{-\pi \cot \theta} < 8 \times 10^{-6}$

(3) maximum damped frequency less than 7.765 rad/s $\qquad$ : $\quad \omega_0 = r \sin \theta < 7.765$

The corresponding parameters of LMI region for above specifications are

$$\alpha_p = 1, r = 30, \theta = 15°$$

Select the weighting matrices $Q = \text{diag}(100, 2000, 10, 300)$ and $R = \text{diag}(4000, 50)$ in the LQR constraint (2.17) for fine tuning. We get the continuous-time controller gain $L$, by YALMIP [60] toolbox accompanying with SDPT3 solver [59], as shown below.

$$L = \begin{bmatrix} 2.8001 & 0.6394 & 1.3587 & -0.0018 \\ -39.5661 & -2.7001 & -0.4673 & 2.3797 \end{bmatrix}$$

The simulation result with an initial condition $x(0) = \begin{bmatrix} -0.262 & 0.349 & 0 & 0 \end{bmatrix}^T$ is shown in Figures 4.2–4.4. We conclude that these controllers can stabilize the original nonlinear system under the required specification.
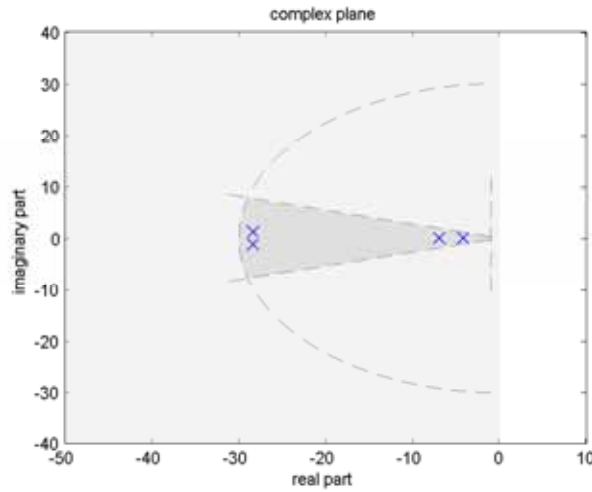


Figure 4.2: Pole location of the closed-loop system

### 4.1.2 Discrete-time controller redesign

We convert the continuous-time controller $L$ in the section 4.1.1 into the discrete-time controller by solving the problem (2.21) for the model that contains the equilibrium point.

$$\begin{aligned}
\min_{Y_d, W_d} \quad & \gamma \\
\text{subject to} \quad & \begin{bmatrix} -Y_d & (A_{d5}Y_d - B_{d5}W_d)^T \\ (A_{d5}Y_d - B_{d5}W_d) & -Y_d \end{bmatrix} < 0 \\
& \begin{bmatrix} -Y_d & (G_{c5}Y_d - A_{d5}Y_d + B_{d5}W_d)^T \\ (G_{c5}Y_d - A_{d5}Y_d + B_{d5}W_d) & -\gamma I \end{bmatrix} < 0
\end{aligned} \tag{4.5}$$

where subscript 5 refers to the discrete-time models obtained from region 5 of PWA model.

We obtain the discrete-time controller gain for sampling period 0.09 s.

$$L_d = \begin{bmatrix} 4.3447 & 3.1230 & -0.2237 & -0.6589 \\ -64.8661 & 3.6038 & 31.6640 & 0.2039 \end{bmatrix}$$

The simulation result in Figure 4.4 shows that both controllers give similar responses and can stabilize the bicycle nonlinear system perfectly. Comparing with the controller designed by classical LQR technique

$$L_{d,LQR} = \begin{bmatrix} 2.6706 & 0.3770 & -0.3630 & -0.4114 \\ -24.6556 & -2.3421 & 16.0030 & 0.2256 \end{bmatrix}$$

This controller gain can stabilize the linearized system. However, the original nonlinear system becomes unstable as shown in Figure 4.3. Moreover, we found that tuning by the classical LQR technique is a difficult task to find the controller gain which can stabilize the system with high nonlinearity over the desired region.

## 4.2   Position control for steering motor

We transform the continuous-time models into the discrete-time models with zero-order-hold method as follows:

Assume the continuous-time model is

$$\begin{aligned} \dot{x}(t) &= Ax(t) + Bu(t) \\ y(t) &= Cx(t) + Du(t) \end{aligned} \tag{4.6}$$

the corresponding discrete-time model with sampling period $T$ is

$$\begin{aligned} x[k+1] &= A_d x[k] + B_d u[k] \\ y[k] &= C_d x[k] + D_d u[k] \end{aligned} \tag{4.7}$$

where

$$\begin{aligned} A_d &= e^{AT} &, \quad B_d &= \int_0^T e^{A\tau} B \, d\tau \\ C_d &= C &, \quad D_d &= D \end{aligned}$$

The design objective is to track a desired position. Let a discrete-time plant of DC motor be described by (4.7) where

$$\begin{aligned} x[k] &= \begin{bmatrix} \theta[k] & \dot{\theta}[k] & I[k] \end{bmatrix}^T \\ y[k] &= \theta[k] = \begin{bmatrix} 1 & 0 & 0 \end{bmatrix} x[k] \end{aligned} \tag{4.8}$$

In order to cancel the steady-state error between the desired position $r[k]$ and the output position $y[k]$, we add the integral state to ensure zero steady-state error as follows:

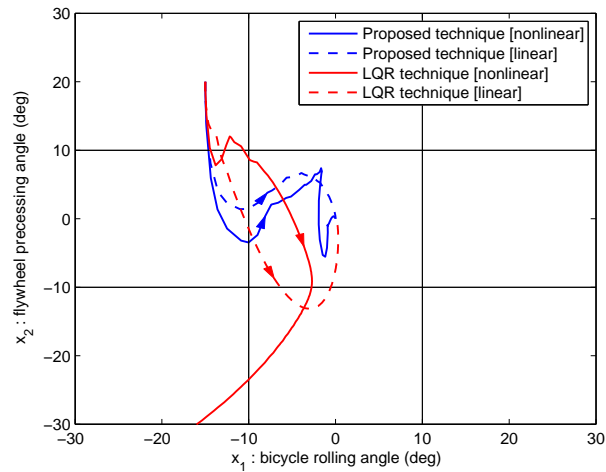$$\begin{aligned} z[k+1] &= z[k] + (r[k] - y[k]) \\ &= z[k] + r[k] - C_d x[k] \end{aligned} \tag{4.9}$$

Figure 4.3: Comparison of the responses between the proposed controller and the classical LQR controller



(a) rolling angle ($x_1$) and precessing angle ($x_2$)

(b) rolling rate ($x_3$) and precessing rate ($x_4$)

(c) yaw rate ($u_1$)
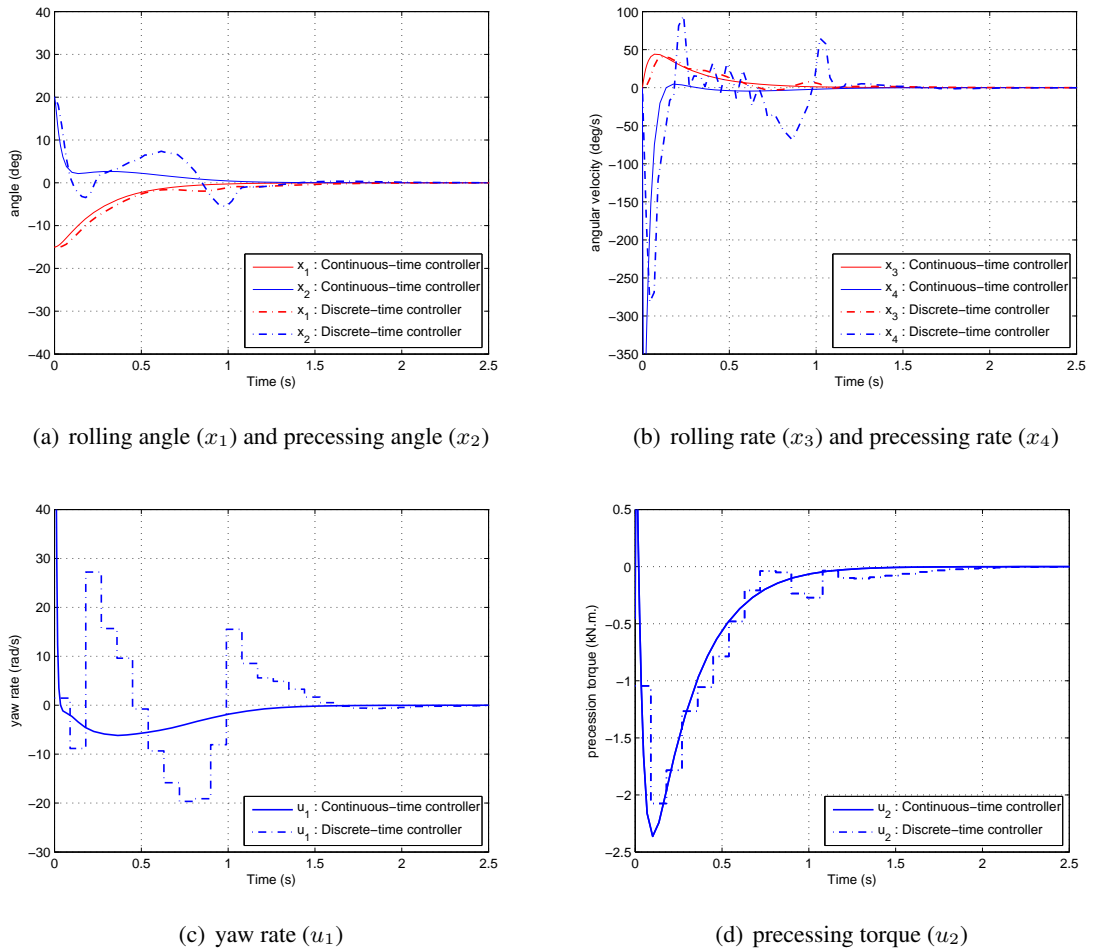
(d) precessing torque ($u_2$)

Figure 4.4: Comparison of the closed-loop responses between continuous-time controller and discrete-time controller

We get the following augmented system.

$$\begin{bmatrix} x[k+1] \\ z[k+1] \end{bmatrix} = \begin{bmatrix} A_d & 0 \\ -C & I \end{bmatrix} \begin{bmatrix} x[k] \\ z[k] \end{bmatrix} + \begin{bmatrix} B_d \\ 0 \end{bmatrix} u[k] + \begin{bmatrix} 0 \\ 1 \end{bmatrix} r[k] \tag{4.10}$$

Let define new variables to measure the difference of steady state value.

$$\begin{aligned} \tilde{x}[k] &\triangleq x[k] - x[\infty] \\ \tilde{z}[k] &\triangleq z[k] - z[\infty] \\ \tilde{u}[k] &\triangleq u[k] - u[\infty] \end{aligned} \tag{4.11}$$

The augmented system in new state variables becomes

$$\begin{bmatrix} \tilde{x}[k+1] \\ \tilde{z}[k+1] \end{bmatrix} = \begin{bmatrix} A_d & 0 \\ -C & I \end{bmatrix} \begin{bmatrix} \tilde{x}[k] \\ \tilde{z}[k] \end{bmatrix} + \begin{bmatrix} B_d \\ 0 \end{bmatrix} \tilde{u}[k] \tag{4.12}$$

Then the present problem is determining the augmented state-feedback matrix

$$\tilde{u}[k] = \begin{bmatrix} F & H \end{bmatrix} \begin{bmatrix} \tilde{x}[k] \\ \tilde{z}[k] \end{bmatrix} \tag{4.13}$$

We design the control law by Linear Quadratic Regulator (LQR) method. The weight matrices $Q, R$ have been selected and find the state-feedback gain that minimizes a quadratic cost function

$$J = \sum_{k=0}^{\infty} \left( \tilde{x}^T[k] Q \tilde{x}[k] + \tilde{u}^T[k] R \tilde{u}[k] \right) \tag{4.14}$$

The solution can be obtained by solving the Ricatti equation which can be solved efficiently via *lqr* function in Matlab software

**Numerical result**

By using the motor specification provided in Table A.2, a continuous-time system of steering motor is described by

$$\frac{d}{dt}\begin{bmatrix} \theta \\ \dot{\theta} \\ I \end{bmatrix} = \begin{bmatrix} 0 & 1 & 0 \\ 0 & -170.45 & 1214.81 \\ 0 & -670.86 & -4775.51 \end{bmatrix} \begin{bmatrix} \theta \\ \dot{\theta} \\ I \end{bmatrix} + \begin{bmatrix} 0 \\ 0 \\ 4.0816 \end{bmatrix} V \tag{4.15}$$

We transform it into discrete-time system with sampling period 0.01 s as

$$\begin{bmatrix} \theta[k+1] \\ \dot{\theta}[k+1] \\ I[k+1] \end{bmatrix} = \begin{bmatrix} 1 & 0.0048 & 0 \\ 0 & 0.1810 & 0.0001 \\ 0 & -0.0264 & 0 \end{bmatrix} \begin{bmatrix} \theta[k] \\ \dot{\theta}[k] \\ I[k] \end{bmatrix} + \begin{bmatrix} 2.9515 \\ 30.4396 \\ 4.2709 \end{bmatrix} V[k] \tag{4.16}$$

The augmented system becomes

$$\begin{bmatrix} \theta[k+1] \\ \dot{\theta}[k+1] \\ I[k+1] \\ z[k+1] \end{bmatrix} = \begin{bmatrix} 1 & 0.0048 & 0 & 0 \\ 0 & 0.1810 & 0.0001 & 0 \\ 0 & -0.0264 & 0 & 0 \\ -1 & 0 & 0 & 1 \end{bmatrix} \begin{bmatrix} \theta[k] \\ \dot{\theta}[k] \\ I[k] \\ z[k] \end{bmatrix} + \begin{bmatrix} 0.0008 \\ 0.1367 \\ 8.5280 \\ 0 \end{bmatrix} V[k] \tag{4.17}$$

Select $Q = \text{diag}(0.1, 10, 10, 50000), R = 800$. We get the controller gain

$$\begin{bmatrix} F & H \end{bmatrix} = -\begin{bmatrix} 85.5021 & 0.4610 & 0.0003 & -5.3381 \end{bmatrix}$$

The simulation results of motor tracking when the desired position is step function and sine function have been shown in figure 4.5
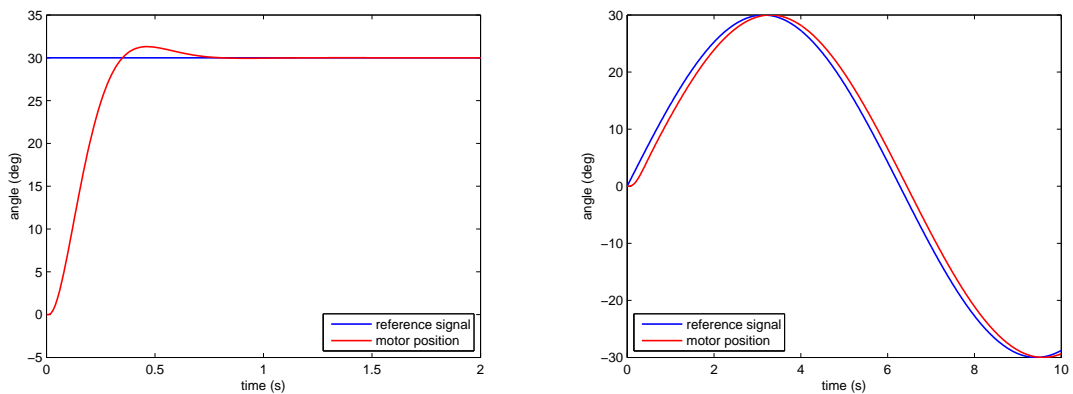


(a) when r[k] =0.5236                    (b) when r[k] =0.5236sin(0.05k)

Figure 4.5: The response of DC motor with tracking controller

# CHAPTER V

# CONTROLLER DESIGN FOR NAVIGATION SYSTEM

In this chapter, we present the algorithm to calculate the steering angle for tracking purpose. Firstly, we introduce the equation for describing a bicycle motion. Then we propose a simple tracking algorithm. After that we will add the complexity in our algorithm step by step for improving its performance.

## 5.1 Bicycle equation of motion

We use the equations of motion proposed in [73] for describing a rear wheel of the bicycle. On the assumptions that the bicycle moves without slipping and the steering axis is perpendicular to the ground, these equations become

$$
\begin{bmatrix} \dot{x}_r \\ \dot{y}_r \\ \dot{\psi} \end{bmatrix} = \sigma \begin{bmatrix} \cos\psi \\ \sin\psi \\ \dfrac{\tan\delta}{b} \end{bmatrix}
\tag{5.1}
$$

where   $(x_r, y_r)$   is the x-y coordinate of rear wheel (m)

         $\psi$        is the yaw angle of rear wheel (rad)

         $\sigma$        is the bicycle speed or rear wheel speed (m/s)

         $\delta$        is the steering angle (rad)

         $b$        is the bicycle wheel base length (m)

After we obtain the position of rear wheel, we can calculate the front wheel position from

$$
\begin{bmatrix} x_f \\ y_f \end{bmatrix} = \begin{bmatrix} x_r \\ y_r \end{bmatrix} + b \begin{bmatrix} \cos\psi \\ \sin\psi \end{bmatrix}
\tag{5.2}
$$

where   $(x_f, y_f)$   is the x-y coordinate of front wheel (m)

## 5.2 Path tracking

To determine the desired steering angle for path tracking purpose, we will use the algorithm which can be divided into 3 steps as follows.

- Step 1: Shifting the coordinate

Suppose we have collected N desired way points $(x_1, y_1), \ldots, (x_N, y_N)$. We transform these way points into the position with respect to a front wheel that represents an observer on the

bicycle by the following equation

$$
\begin{bmatrix} x_i' \\ y_i' \end{bmatrix} = \begin{bmatrix} \cos\psi & \sin\psi \\ -\sin\psi & \cos\psi \end{bmatrix} \begin{bmatrix} x_i - x_f \\ y_i - y_f \end{bmatrix}
\tag{5.3}
$$

- Step 2: Searching the nearby way points

  For a convenience in explanation, we will consider way points $(x_i', y_i')$ as the coordinate on complex plane $z_i' = x_i' + jy_i' = |z_i'|\angle\theta_i'$. We select the way points that satisfy the following criteria

$$
|z_i'| \leq S_{rad} \text{ and } |\theta_i'| \leq S_{ang}
\tag{5.4}
$$

  where $S_{rad}$ is the maximum searching radius, $S_{ang}$ is the maximum searching angle. With these parameters, we can imply that the desired steering angle doesn't exceed $S_{ang}$.
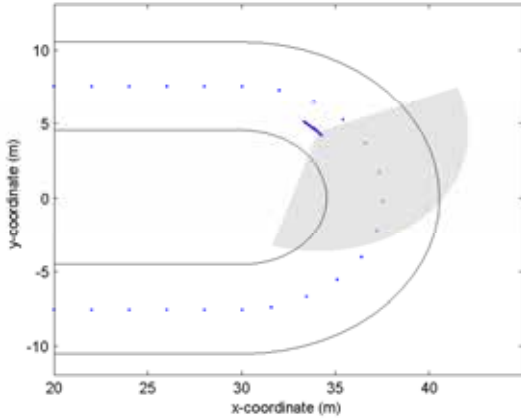


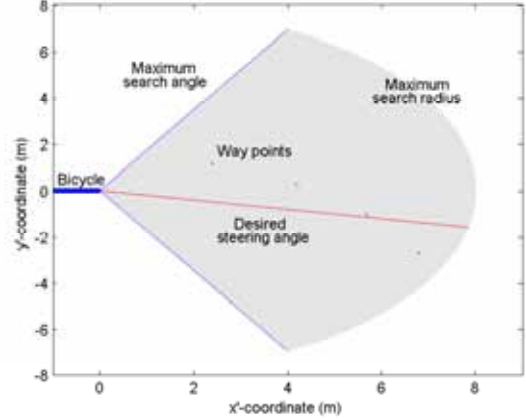Figure 5.1: Bicycle on a global coordinate



Figure 5.2: View of the observer on the bicycle

- Step 3: Calculating the desired steering angle for path tracking purpose

  We find a straight line, described by $y' = \hat{m}x'$, that fits to the nearby way points obtained in step 2 and pass through the front wheel position. We use linear regression using least square error technique for finding the parameter $m$ as the following optimization problem.

$$
\hat{m} = \operatorname*{argmin}_{m} \left\| \begin{bmatrix} y_1' \\ y_2' \\ ... \\ y_n' \end{bmatrix} - m \begin{bmatrix} x_1' \\ x_2' \\ ... \\ x_n' \end{bmatrix} \right\|
\tag{5.5}
$$

  where $(x_1', y_1'), ..., (x_n', y_n')$ are the nearby way points obtained in step 2.

  The closed form solution is

$$
\hat{m} = \frac{\sum\limits_{i=1}^{n} x_i' y_i'}{\sum\limits_{i=1}^{n} x_i'^2}
\tag{5.6}
$$

Finally, we get a desired steering angle.

$$\delta_{track} = \arctan \hat{m} \tag{5.7}$$

We generate a map and way points in the simulation and then test our algorithm. The simulation result shows the bicycle can move along the desired path. However, there are some distance errors when moving along the curvature path but it's acceptable as long as it doesn't run out of the track.

## 5.3 Simulation setup

We generate a map like an athletics track that includes two straight line paths and two semicircular paths as shown in Figure 5.3. Way points are laid on the desired path described by

$$(x(t), y(t)) = \begin{cases} (t, 7.5) & 0 \leq t \leq 30 \\ (30 + 7.5 \sin(\pi(\frac{t-30}{30})), 7.5 \cos(\pi(\frac{t-30}{30}))) & 30 \leq t \leq 60 \\ (90 - t, -7.5) & 60 \leq t \leq 90 \\ (-7.5 \sin(\pi(\frac{t-90}{30})), -7.5 \cos(\pi(\frac{t-90}{30}))) & 90 \leq t \leq 120 \end{cases} \tag{5.8}$$

These way points are located with 2 meters equally space on a middle track between an inner track and an outer track. The width of this track is 6 meters.
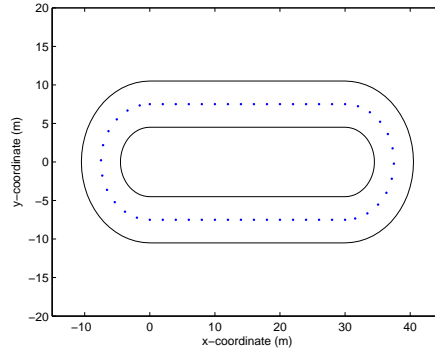


Figure 5.3: Map with the desired way points

We simulate a bicycle trajectory with an update period 0.09 s. for $\delta_{filter}$ (the same period as the control signal of the stabilizing system) and 0.5 s. for $\delta_{desired}$ obtained from path tracking algorithm. Note that the update period of $\delta_{desired}$ must be greater than 0.2 s. due to the limitation of GPS.

## 5.4 Steering signal filter

With our proposed path tracking method, the desired steering angle will suddenly change when some way points are added or removed from searching algorithm. So we smoothen this signal with a following equation.

$$\delta_{filter}[k] = \delta_{filter}[k-1] + w_{filter}(\delta_{desired}[k] - \delta_{filter}[k-1]) \tag{5.9}$$

where $w_{filter}$ is the filter weight. The comparison of the signal with 2 different filter weights are shown in Figure 5.4



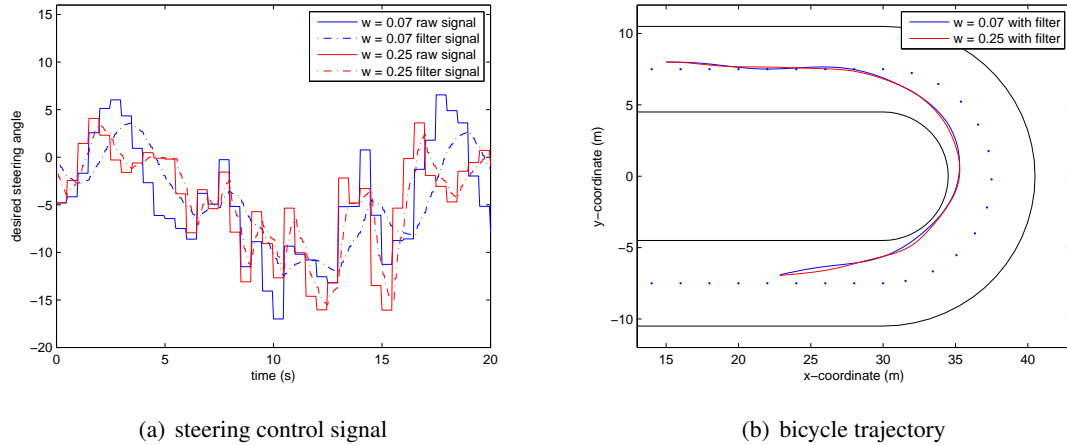(a) steering control signal  (b) bicycle trajectory

Figure 5.4: Comparison of the responses with different filter weights

Since the bicycle model in section 3.1.1 is derived under the assumption that a steering angular velocity is small, we must avoid to changing the steering angle too fast. So we select the parameter $w_{filter} = 0.07$ for our algorithm.

## 5.5 Effect of the searching radius and searching angle

There are two adjustable parameters in our path tracking algorithm. We will show the effect of the variation of these parameters in this section.

- Searching radius ($S_{rad}$)

  Searching radius parameter determines how far we have to consider the way points in front of the bicycle. If this parameter is small, a bicycle trajectory will be oscillated. If this parameter is high, a bicycle trajectory will be smooth especially for a straight path, but it may move too close to the inner track of a circular path as shown in Figure 5.5

- Searching angle ($S_{ang}$)

  Searching angle parameter determines how wide we have to consider the way points from a heading direction of the bicycle. This parameter seems not to affect a bicycle trajectory as shown in Figure 5.5. However, the effect is arise in the noisy system as shown in Figure 5.6. If this parameter is small, the bicycle will run out of the track because it cannot detect the way points. If this parameter is high, the tracking algorithm will be more reliable but the desired steering angle will be high.

So we select the parameters $S_{rad} = 8$ and $S_{ang} = 65°$ for our algorithm because it works well on the simulation even in the noisy system.
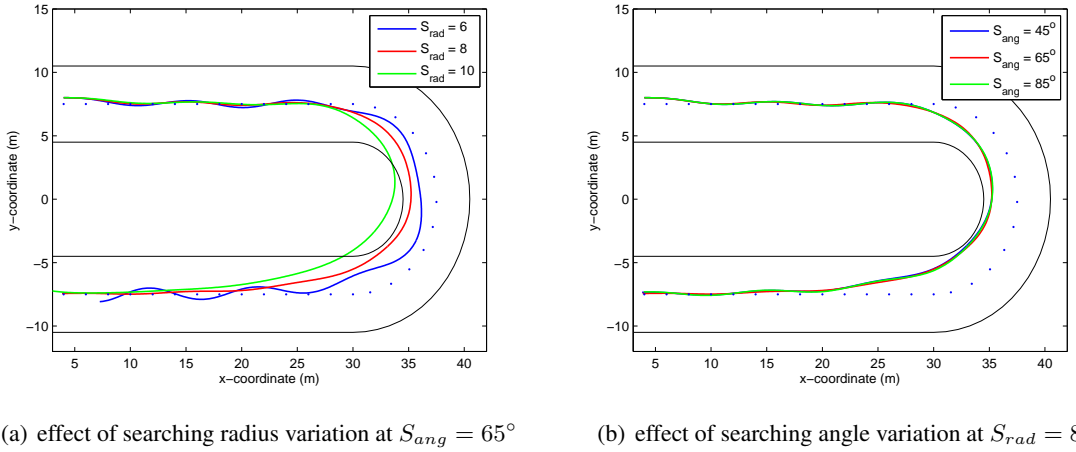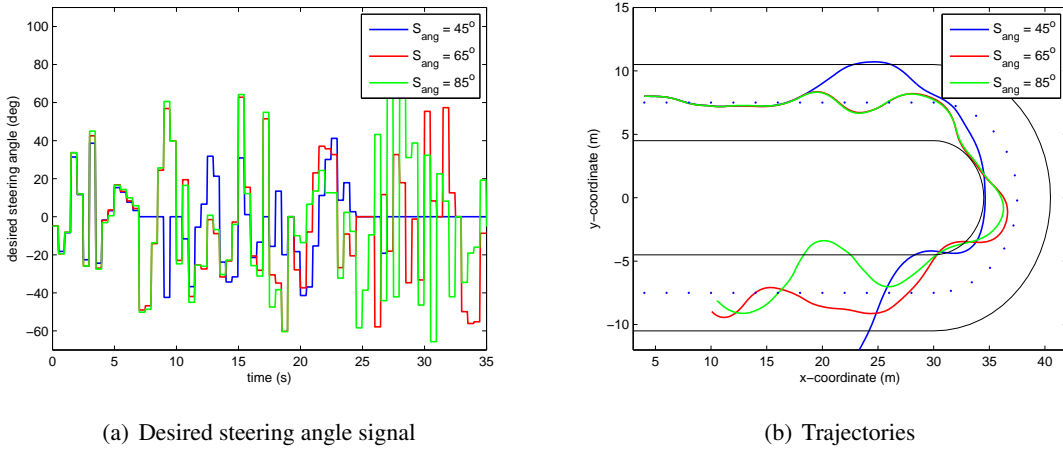
(a) effect of searching radius variation at $S_{ang} = 65°$

(b) effect of searching angle variation at $S_{rad} = 8$

Figure 5.5: Comparison of the trajectories with different searching parameters



(a) Desired steering angle signal

(b) Trajectories

Figure 5.6: Comparison of the responses in noisy system with different angle searching at $S_{rad} = 8$

## 5.6 GPS Filter

Since a GPS has an uncertainty in its measurement, we will use a position estimator instead of a measured data to calculate a desired steering angle for tracking purpose. We use Extended Kalman Filter (EKF) [70] to estimate the position of rear wheel as follows.

From the equation of motion (5.1), we get a discrete-time model with sampling period $T_{navi}$

$$x[k] = f(x[k-1], \delta[k-1], w[k-1]) = x[k-1] + \begin{bmatrix} \sigma \cos \psi[k-1] \\ \sigma \sin \psi[k-1] \\ \dfrac{\sigma}{b} \tan \delta[k-1] \end{bmatrix} T_{navi} + w[k] \quad (5.10)$$

with a measured state

$$z[k] = x[k] + v[k] \quad (5.11)$$

where $x = \begin{bmatrix} x_r & y_r & \psi \end{bmatrix}^T$ is the state variable, $w$ and $v$ are random variables that represent the process noise and the measurement noise. They are assumed to be Gaussian random variables with probability distributions $N(0, Q)$ and $N(0, R)$ respectively.

Then we obtain the EKF algorithm as shown below

- Prediction step

Prior estimated state: $\quad\quad\quad\quad\quad\quad \hat{x}^-[k] = f(\hat{x}[k-1], \delta[k-1], 0)$ $\quad\quad\quad$ (5.12)

Prior estimate error covariance: $\quad\quad \hat{P}^-[k] = A[k-1]\hat{P}[k-1]A^T[k-1] + Q$ $\quad$ (5.13)

- Correction step

Kalman gain: $\quad\quad\quad\quad\quad\quad\quad K[k] = \hat{P}^-[k](\hat{P}^-[k] + R)^{-1}$ $\quad\quad\quad$ (5.14)

Posterior estimated state: $\quad\quad\quad \hat{x}[k] = \hat{x}^-[k] + K[k](z[k] - \hat{x}^-[k])$ $\quad\quad$ (5.15)

Posterior estimate error covariance: $\quad \hat{P}[k] = (I - K[k])\hat{P}^-[k]$ $\quad\quad\quad$ (5.16)

where $\quad A \quad$ is the Jacobian matrix of partial derivatives of $f$ with respect to $x$,

$$A[k-1] = \begin{bmatrix} 1 & 0 & -T_{navi}\sigma\sin\hat{\psi}[k-1] \\ 0 & 1 & T_{navi}\sigma\cos\hat{\psi}[k-1] \\ 0 & 0 & 1 \end{bmatrix}$$

$Q \quad$ is the process noise covariance

$R \quad$ is the measurement noise covariance

We assume that the measured data is obtained by quantizing the actual bicycle position plus gaussian noise with zero mean and variance 5 m$^2$. The quantizing resolution for x-position and y-position is 0.18 and 0.185 m. respectively. These resolutions are determined by the resolution of GPS measuring around the faculty of engineering, Chulalongkorn university. (Latitude $13°14.2647'$N, Longitude $100°31.9049'$E) Then we simulate the bicycle trajectory using the parameters $Q = $ diag(0.005, 0.005, 0.5) and $R = $ diag$(5, 5, 0.005)$ from the simulink diagram in Figure 5.8. The simulation results show that the algorithm with EKF provide a better performance in Figure 5.7.
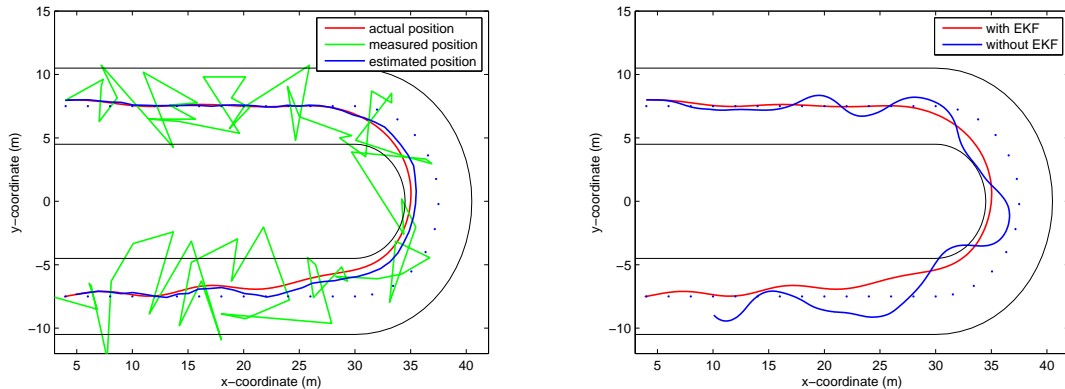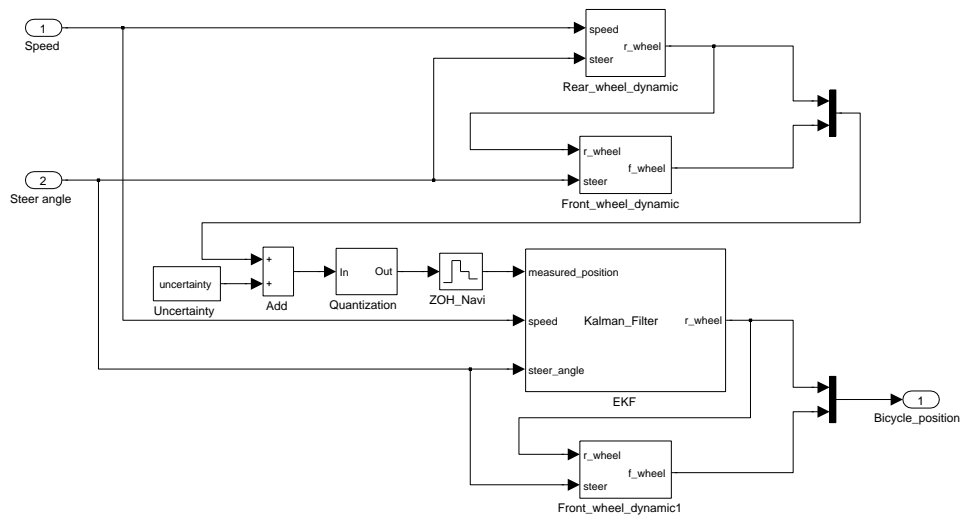


(a) Desired steering angle signal $\quad\quad\quad\quad\quad\quad\quad\quad\quad$ (b) Trajectories
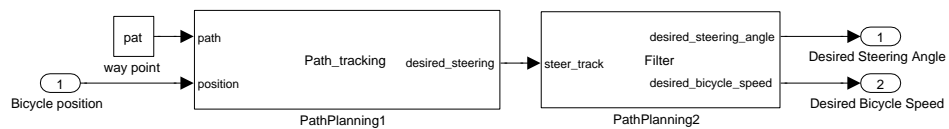
Figure 5.7: Comparison of the trajectories in noisy system with EKF implementation
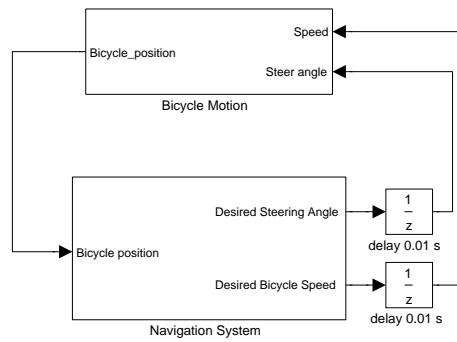
(a) overview of the system



(b) bicycle motion subsystem



(c) navigation subsystem

Figure 5.8: Simulink diagram for the tracking system

# CHAPTER VI

# INTEGRATION OF THE STABILIZATION
# AND THE NAVIGATION SYSTEM

In chapter 4–5, we have designed the controller for the stabilizatiion system and navigation system separately. Unfortunately, the control signal of these systems has the desired steering angle as a common variable. To combine them together, we need to recalculate the desired steering angle that can track a desired path while maintaining the bicycle to stay upright.

## 6.1 Compromise algorithm

Suppose we get the desired steering angle for tracking purpose $\delta_{track}$ and the desired steering angle for stabilizing purpose $\delta_{stat}$. We will recalculate with the following equation.

$$\delta_{actual} = w_{stat}\delta_{stat} + (1 - w_{stat})\delta_{track} \tag{6.1}$$

where $w_{stat} \in [0, 1]$. We also define a tracking cost for indicating a tracking performance and a stabilizing cost for indicating a stabilizing performance as follows.

**Definition 6.1.** *Tracking cost*
*Let $e_{track}(t)$ be a shortest distance measured from a desired path to a rear wheel of a bicycle at time t. The tracking cost over time $t = 0$ to $t = T$ is defined by*

$$J_{track} = \int_0^T e_{track}^2(t)dt \tag{6.2}$$

**Definition 6.2.** *Stabilizing cost (or State cost)*
*Let $e_{stat}(t)$ be a the different of a present rolling angle and a rolling angle of an equilibrium point at time t. The stabilizing cost over time $t = 0$ to $t = T$ is defined by*

$$J_{stat} = \int_0^T e_{stat}^2(t)dt \tag{6.3}$$

The simulation results with weighting parameter $w_{stat}$ 0.2, 0.3, 0.4 and 0.5 have been shown in Figure 6.2–6.5. The comparison of the tracking cost and stabilizing cost for different weight is provided in Table 6.1.

According to the simulation results, we found that the higher weighting parameter $w_{stat}$ tends to give a better stabilizing performance. However, this statement is not true when we continue to increase the weighting parameter from 0.4 to 0.5.

In more detail, when the weighting parameter is too small, the gyroscopic flywheel must stabilize the bicycle alone. So the flywheel precessing angle will be shifted from the equilibrium point until the gyroscopic flywheel cannot produce torque to stabilize the bicycle. As a result, the bicycle will fall down. On the contrary, if the weighting parameter is too high, the tracking performance will be degraded and the tracking system will provide the high desired steering angle. These incidents make the system oscillate, especially when the bicycle almost runs out of the track, and also cause the bicycle to fall down.

Table 6.1: Comparison of the tracking cost and the stabilizing cost

| Weight ($w_{stat}$) | Total time | Average tracking cost | Average stabilizing cost |
|---|---|---|---|
| 0.2 | 38.10 s. [Failure] | 0.8023 | 0.01358 |
| 0.3 | 50.00 s. | 0.6306 | 0.00202 |
| 0.4 | 50.00 s. | 0.2796 | 0.00146 |
| 0.5 | 39.30 s. [Failure] | 1.4162 | 0.00975 |

## 6.2   Effect of a delay time in steering control

In the previous section, we assume that the steering angle is delayed from the actual desired steering angle in 0.01 s. (If we set the delay time to 0 s., the Simulink program will crash an algebraic loop problem.) In this section, we will add the steering motor dynamic into the simulation and show the results.

We assume the steering dynamic is described by the second order model of steering motor in (4.15). The simulink diagram of steering system, contains the plant of motor and $\pm 12$ volt saturation block for limiting the control input, is shown in Figure 6.6. Suppose that the bicycle is moving at a constant speed in a steady state. Then we can neglect the driving motor dynamic in the simulation. We simulate the bicycle trajectory as provided in Figure 6.7–6.10 by using three types of steering dynamic in Table 6.2.

The simulation result shows that a steering controller with the settling time 0.5 s. and small overshoot (type A) give an excellent result for the overall system. The type B controller gives a poor result due to its slow response. The type C controller makes a system oscillate due to its high overshoot response and lead the bicycle system to be unstable even if it has the same settling time of type A controller.
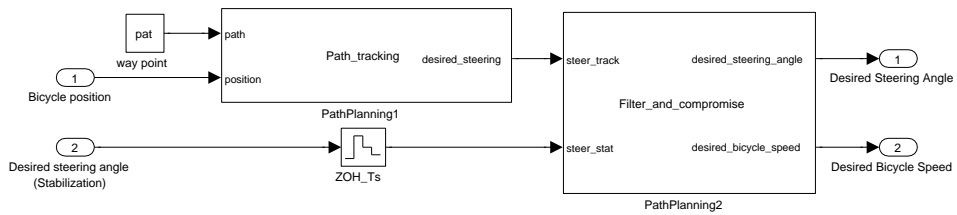
Table 6.2: Types of steering controller

| Type | Controller gain in equation (4.13) | Settling time (5 %) | Overshoot |
|------|-----------------------------------|---------------------|-----------|
| A | $-\begin{bmatrix} 85.5021 & 0.4610 & 0.0003 & -5.3381 \end{bmatrix}$ | 0.5 s. | 6.20 % |
| B | $-\begin{bmatrix} 24.3932 & 0.1392 & 0.0001 & -0.4792 \end{bmatrix}$ | 1.0 s. | 4.32 % |
| C | $-\begin{bmatrix} 108.5533 & 0.5732 & 0.0004 & -8.3230 \end{bmatrix}$ | 0.5 s. | 16.70 % |
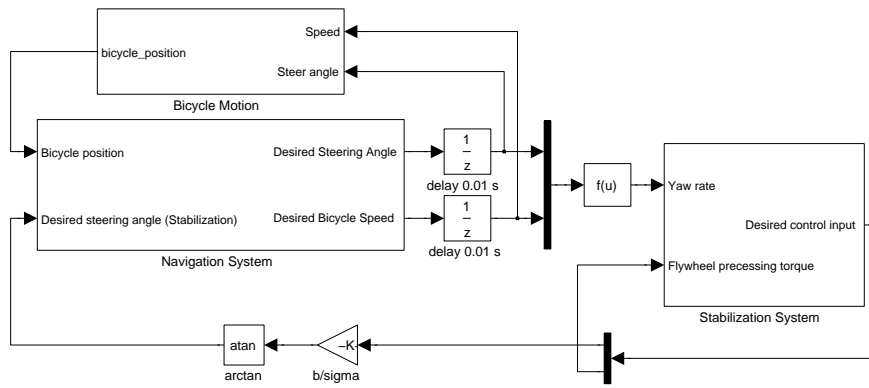
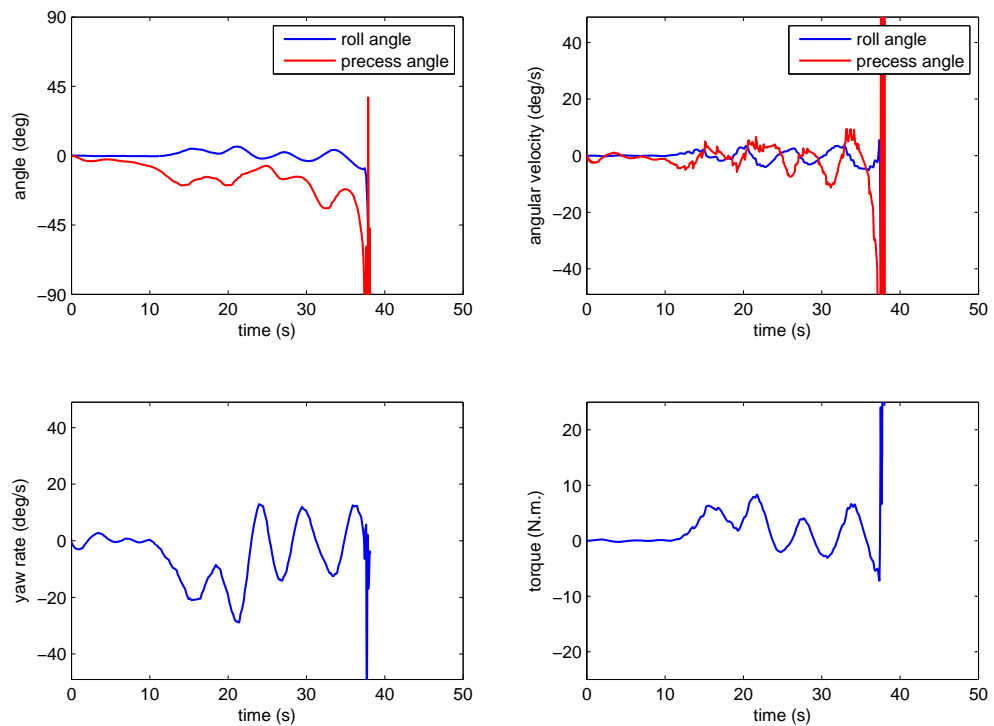(a) overview of the system
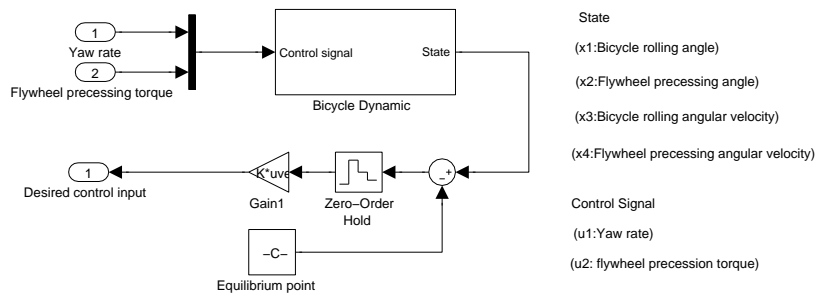


(b) stabilization subsystem



(c) navigation subsystem

Figure 6.1: Simulink diagram for the integrated stabilization and navigation system
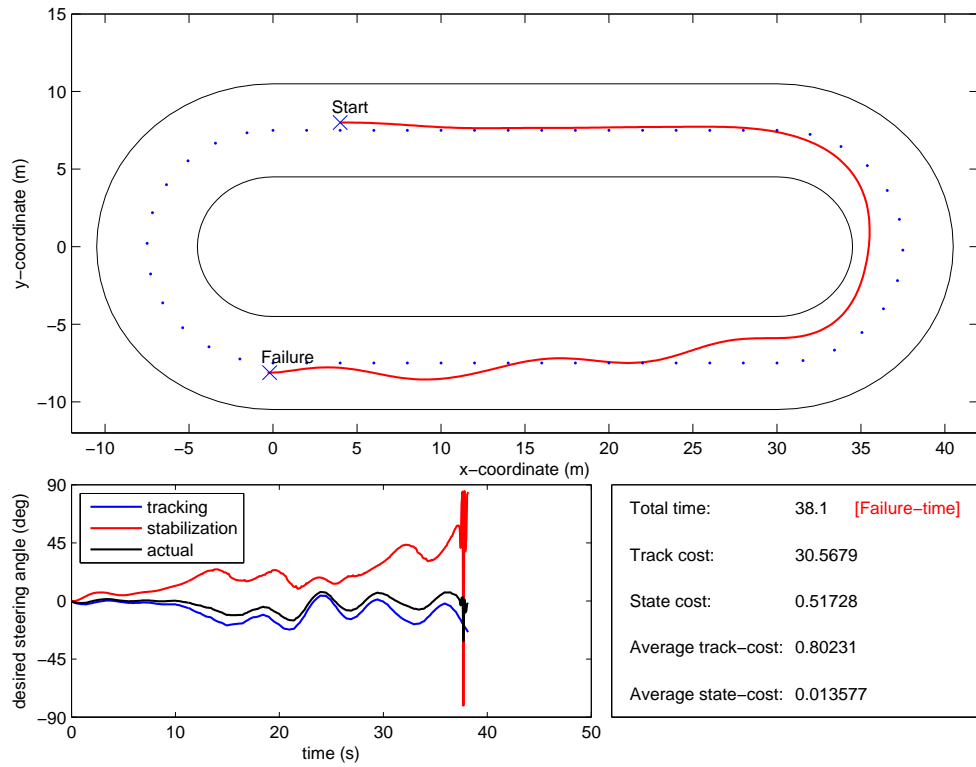
(a) bicycle trajectory and steering control signal



(b) state responses and control signals

Figure 6.2: Simulation result for the weighting parameter $w_{stat} = 0.2$

(a) bicycle trajectory and steering control signal



(b) state responses and control signals

Figure 6.3: Simulation result for the weighting parameter $w_{stat} = 0.3$

(a) bicycle trajectory and steering control signal
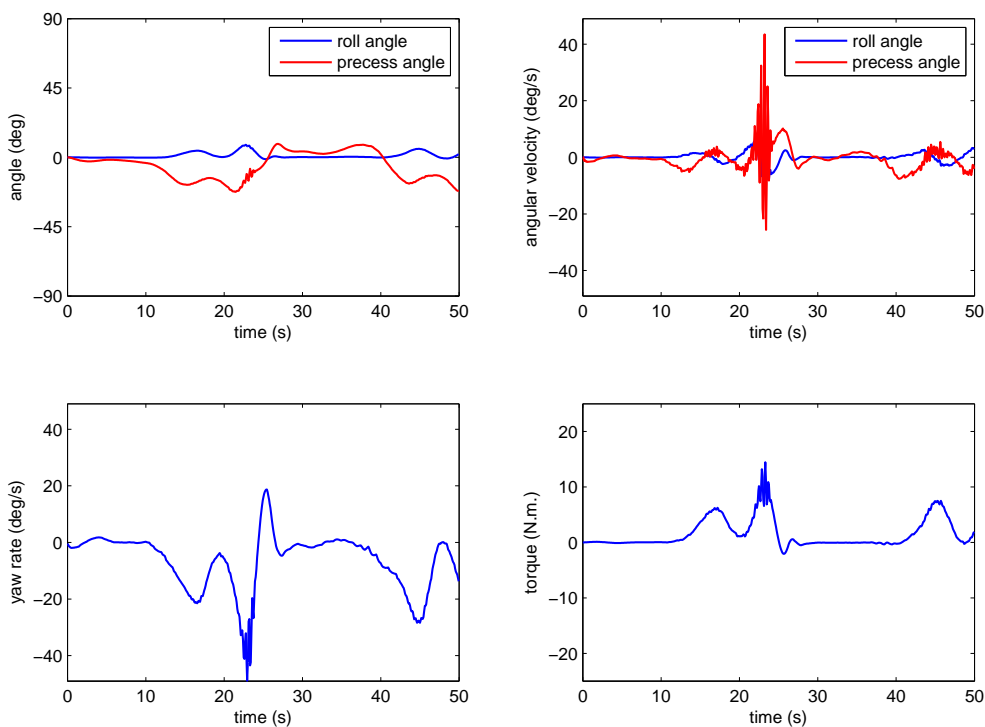


(b) state responses and control signals

Figure 6.4: Simulation result for the weighting parameter $w_{stat} = 0.4$

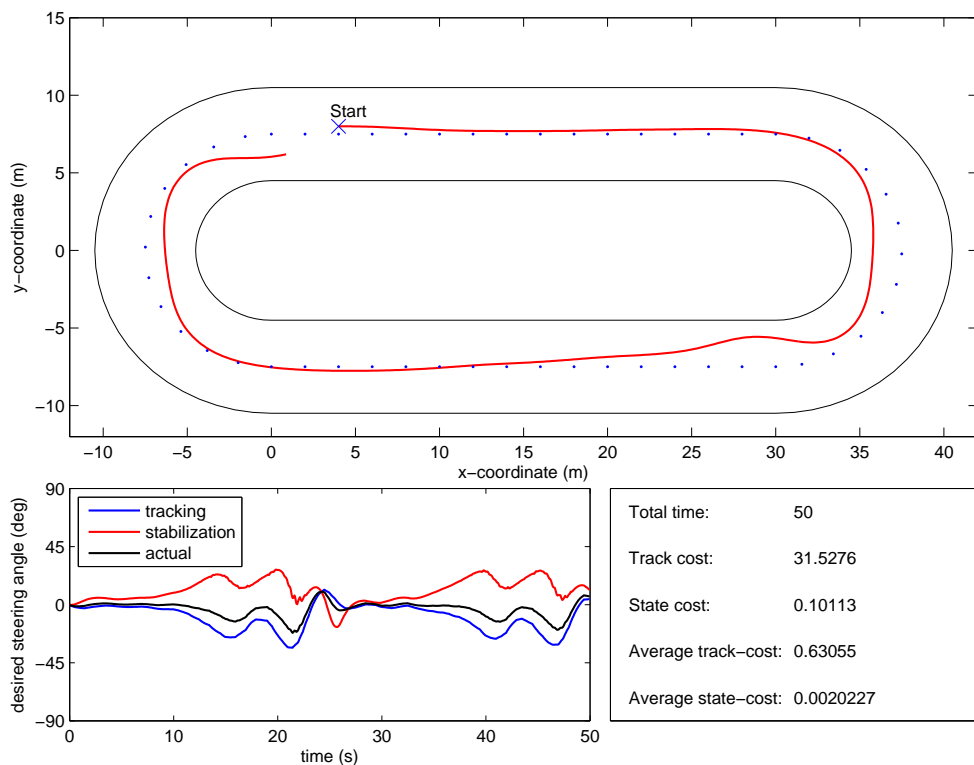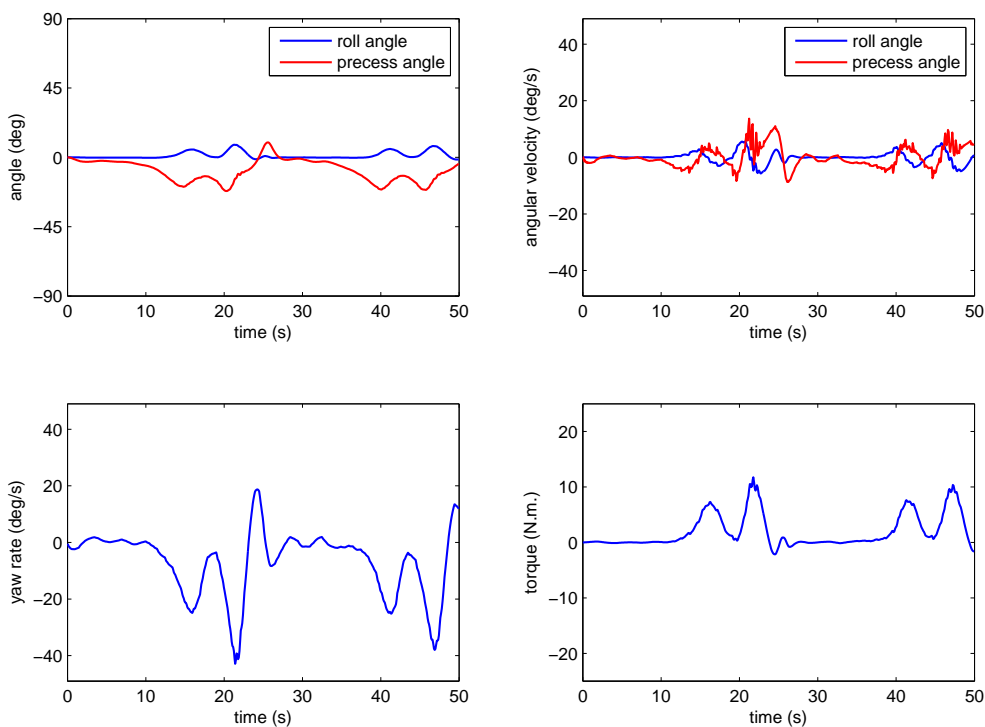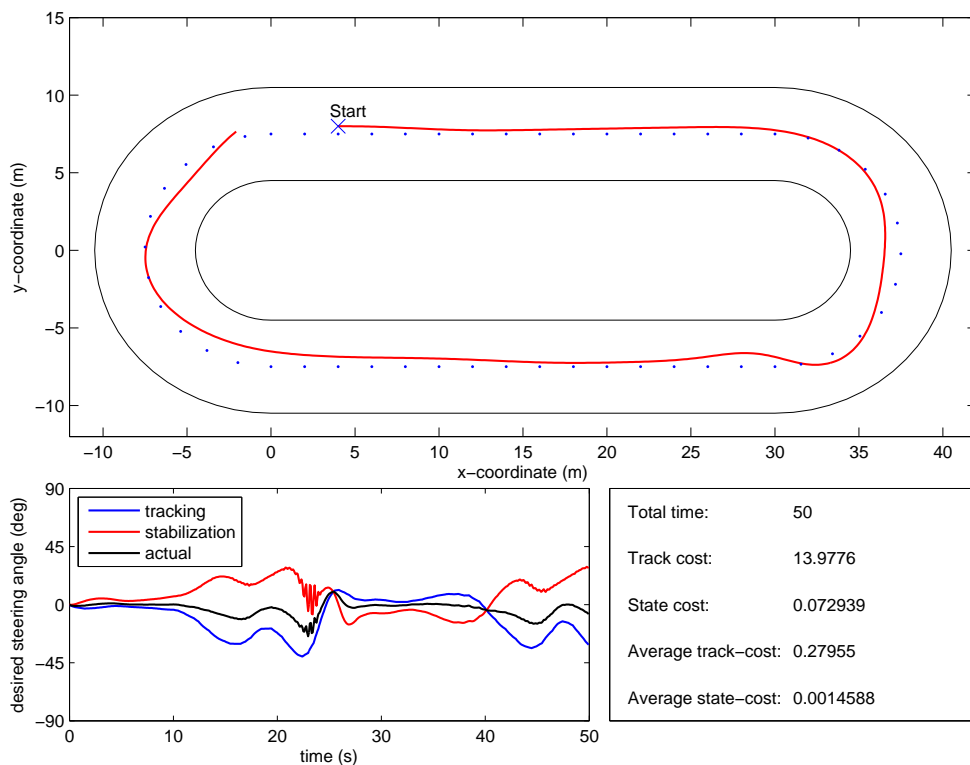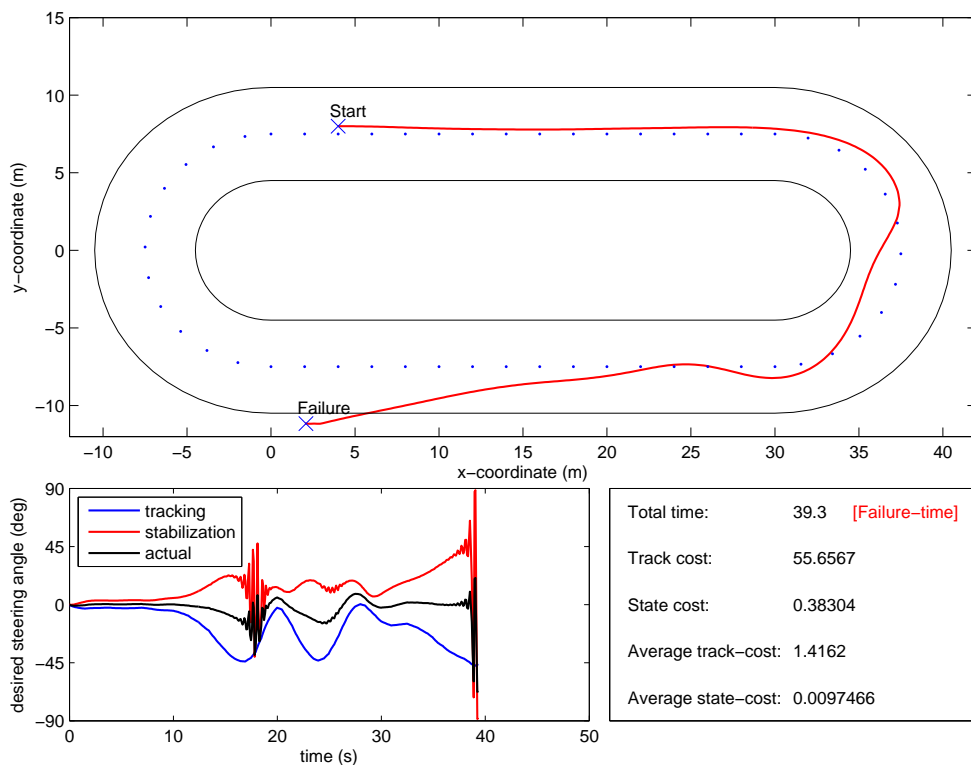(a) bicycle trajectory and steering control signal
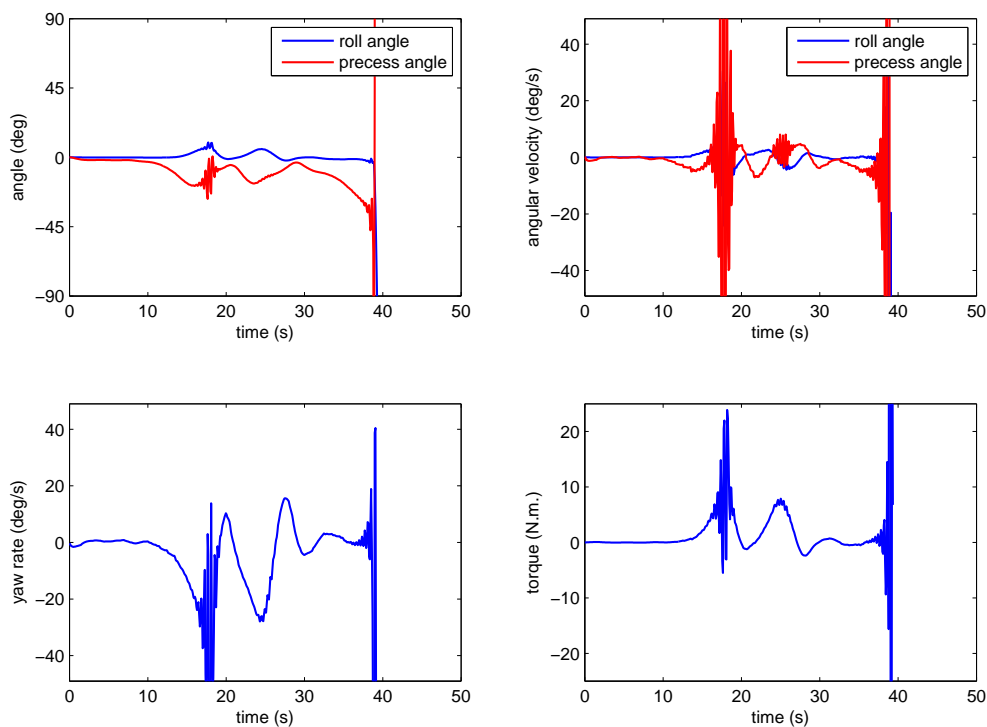


(b) state responses and control signals

Figure 6.5: Simulation result for the weighting parameter $w_{stat} = 0.5$
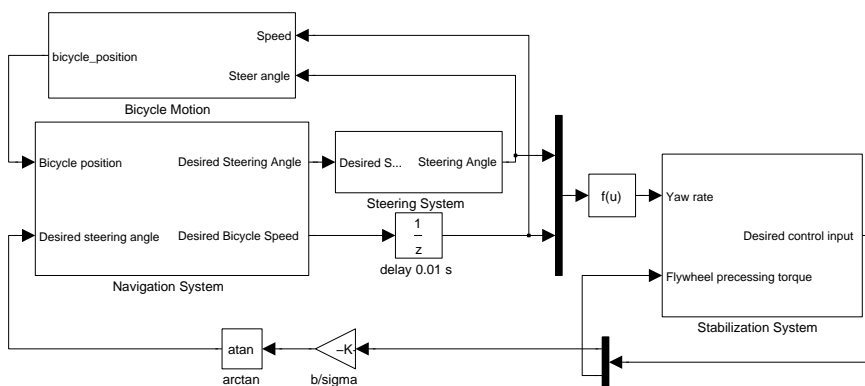
(a) overview of the system
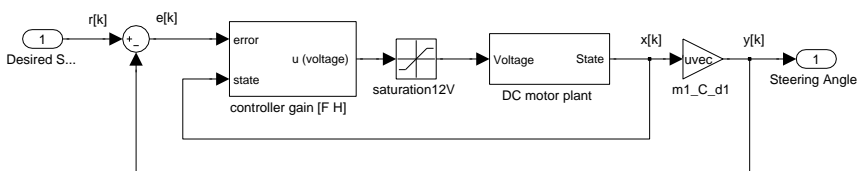


(b) steering subsystem

Figure 6.6: Simulink diagram for the integrated stabilization and navigation system with an additional steering system

Figure 6.7: Simulation result for the weighting parameter $w_{stat} = 0.4$ with type A steering controller



Figure 6.8: Simulation result for the weighting parameter $w_{stat} = 0.4$ with type B steering controller

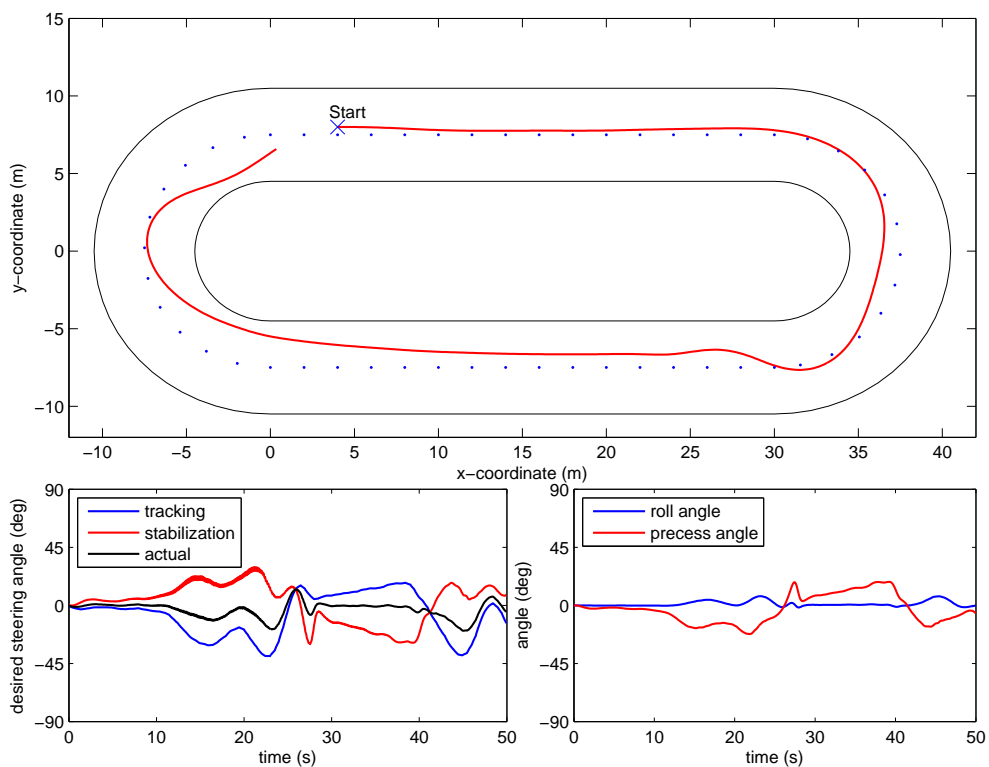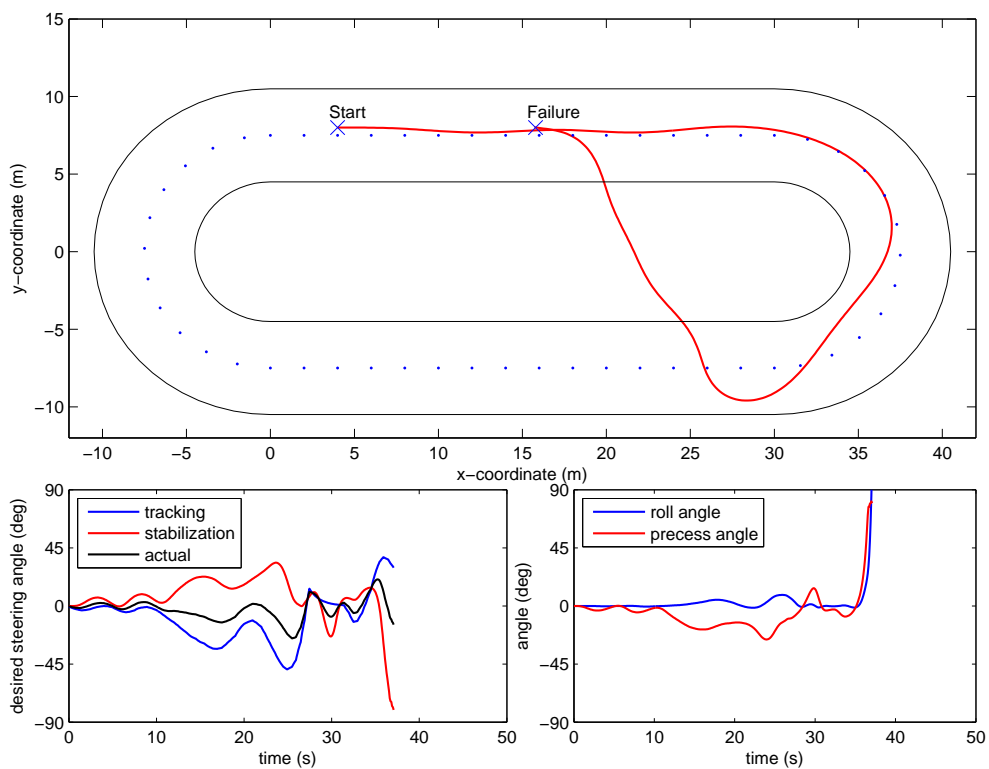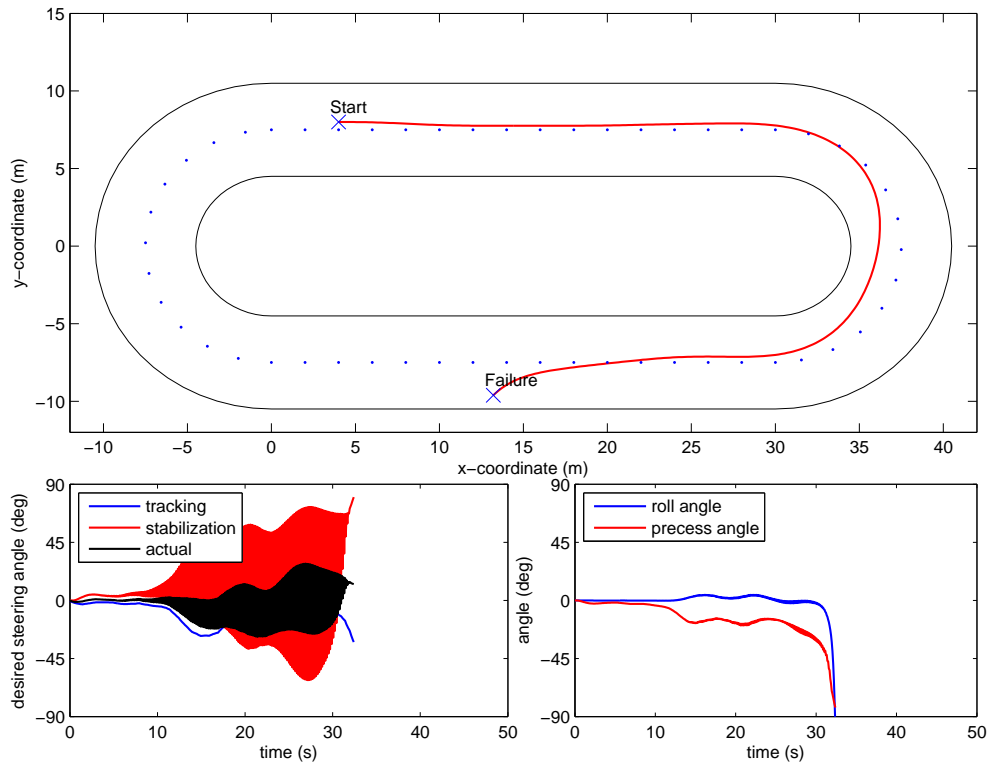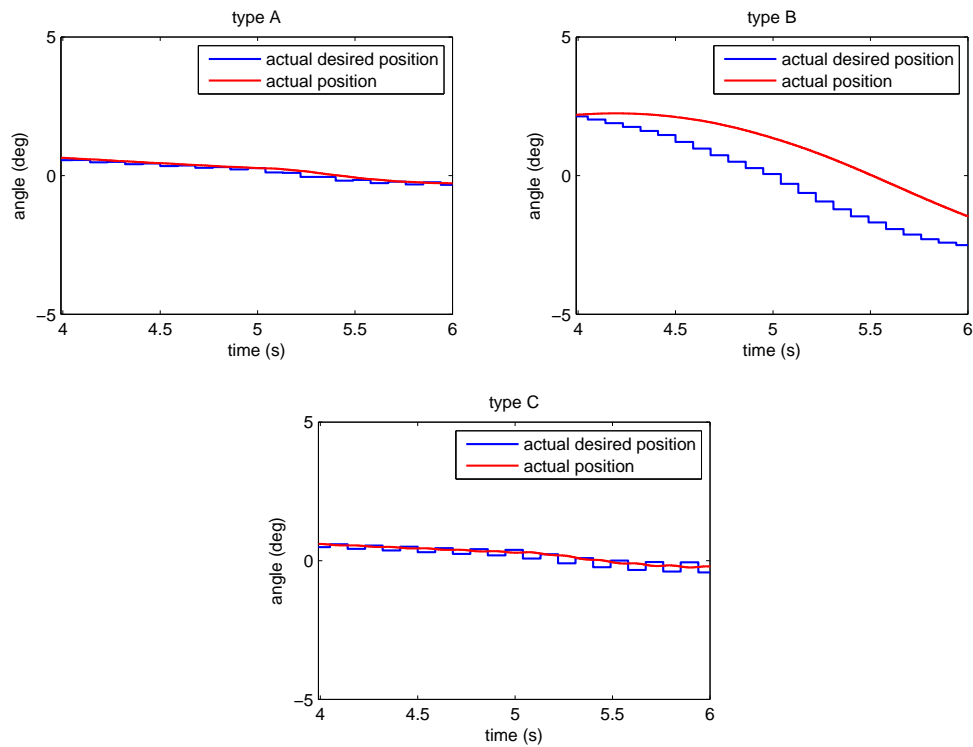Figure 6.9: Simulation result for the weighting parameter $w_{stat} = 0.4$ with type C steering controller



Figure 6.10: Steering response from each type of steering controller

# CHAPTER VII

# CONCLUSIONS

## 7.1  Summary

In this thesis, we present the design of an unmanned bicycle that can stay upright while following the path autonomously in a computer simulation. The bicycle consists of two main systems; stabilization system and navigation system. We design each system separately and combine them together. We develop a novel stabilization technique for unmanned bicycle which utilizes not only the gyroscopic stabilization but also incorporating the steering control for an intelligent bicycle robot. To design a controller for stabilizing the bicycle, we design a state-feedback controller which guarantees the stability of a class of nonlinear systems over the desired region and ensures some practical performance criteria of the closed-loop system. We apply the piecewise affine technique together with the regional pole placement and linear quadratic regulator in order that all design formulations are cast as a linear matrix inequalities optimization problem. The discrete-time controller is also obtained from the continuous-time controller via LMI approach. The controller design for navigation system is obtained by applying a linear regression using least square error method. An integrated stabilization and navigation system of the bicycle has been design. Since the control signal of the stabilization system and the navigation system has a common variable; desired steering angle, we propose the compromise algorithm for recalculating this control signal when we integrate both systems together.

Chapter 1 contains a research motivation. A literature review on piecewise affine (PWA) systems and bicycle dynamic & control is provided. Many researches on PWA work about model representations, system identifications and controller designs. For the literature review on a bicycle, it covers the bicycle dynamic model and bicycle stabilization method. Then we present an objective, a scope and contributions of this thesis.

Chapter 2 briefly introduce the background knowledges of Linear matrix inequality (LMI) and Piecewise affine (PWA) system. A great advantage of LMI techniques is various design techniques can be combined via LMI. Then, some control design strategies formulated in LMI constraints have been shown. All of these techniques will be used to design a controller for stabilizing the bicycle in chapter 4.

In chapter 3, the models of each subsystem of the bicycle are provided. The bicycle nonlinear model for both steering and gyroscopic stabilization has been proposed. We show some behavior analyses of this bicycle such as a bicycle dynamic, a linearized model and a piecewise affine model. DC motor model is also provided because it contains in a bicycle mechanism.

In chapter 4, the state-feedback controller design with performance improvement for piecewise affine system has been proposed. The controller synthesis is performed by solving the optimization problem under LMI constraints which combine regional pole placement for coarse tuning, LQR for fine tuning and piecewise quadratic stabilization to guarantee the stability over the desired region. Moreover, the discrete-time controller is also obtained via LMI approach. This proposed design method is applying to find the controller for stabilizing the bicycle.

In chapter 5, the controller design for tracking purpose has been developed. The desired steering angle is calculated base on a linear regression using least square error method. Some digital filters, including integral filter and Extended Kalman Filter, are applied to improve the effectiveness of tracking algorithm in noisy systems. The effect of the variation of adjustable parameters in the proposed algorithm has been illustrated.

In chapter 6, we propose the compromise algorithm for weighting the control signal of the integrated stabilization and navigation system since the control signal of these systems has desired steering angle as a common variable. The simulation result for different weight has been shown. Afterward, the delay time due to a steering motor is taken into account.

Finally, the results from each chapter have been discussed and we give a future work guideline at the end.

## 7.2  Future work guideline

1. *Development of bicycle model for both steering and gyroscopic stabilization*
   The bicycle nonlinear model for both steering and gyroscopic stabilization in chapter 3 has been derived under the assumption that the steering angular velocity must be small. So we can neglect the front fork dynamic of the bicycle. However, this model may describe the bicycle dynamic inaccurately in practice when this assumption is violated.

2. *PWA observer of an unmanned bicycle using gyroscopic effect*
   We have assumed that all bicycle states of stabilization system are measurable. So we don't design an observer for this system. Even though we don't use an observer for the stabilization system, it works well because we don't take the uncertainty into account. In case of noisy systems, we should implement the PWA observer to reduce noise for better performance.

3. *Implementation on the real bicycle*
   All of the results in this thesis have been illustrated via the computer simulation. However, these results should be verified by implementing the proposed controller on the experimental bicycle. We have tested some functions on the bicycle prototype but it is still not complete due to the mechanical problem.

# REFERENCES

[1] Whipple, F. J. W. The stability of the motion of a bicycle. Quarterly Journal of Pure and Applied Mathematics 30, 120 (1899) : 312–348.

[2] Getz, N., and Marsden, J. Control for an autonomous bicycle. in Proceedings of the IEEE International Conference on Robotics and Automation, vol. 2. May 1995.

[3] Yamakita, M., and Utano, A. Automatic control of bicycles with a balancer. in Proceedings of the IEEE/ASME International Conference on Advanced Intelligent Mechatronics, pp. 1245–1250, July 2005.

[4] Spry, S. C., and Girard, A. R. Gyroscopic Stabilization of Unstable Vehicles: Configurations, Dynamics, and Control. March 2008. (Unpublished Manuscript)

[5] Keo, L., and Yamakita, M. Controller design of an autonomous bicycle with both steering and balancer controls. in Proceedings of the IEEE Control Applications and Intelligent Control, pp. 1294–1299, July 2009.

[6] Lowell, J., and McKell, H. D. The stability of bicycles. American Journal of Physics 50, 12 (1982) : 1106–1112.

[7] Schwab, A. L. Dynamics of flexible multibody systems. Doctoral dissertation, Royal Institute of Technology, 2002.

[8] Lesser, M. The analysis of complex nonlinear mechanical systems, a computer algebra assisted approach, of world scientific series on nonlinear science–Series A. Singapore:, World Scientific, vol. 17, 1995.

[9] Elmqvist, H., Mattsson, S. E. and Otter M. Modelica a language for phsical system modeling, visualization and interaction. in Proceedings of IEEE Symposium on Computer-Aided Control System and Design, CACSD'99, Hawaii, August 1999.

[10] Anon. Autosim 2.5+. Mechanical Simulation Corp. Technical Report. Ann Arbor, MI, 1998.

[11] Roland, R. D. Computer simulation of bicycle dynamics. in Proceedings of ASME Symposium on Mechanics Sport, pp. 35–83, 1973.

[12] Limebeer, D., and Sharp, R. Bicycles, motorcycles, and models. IEEE Control Systems Magazine 26 (October 2006): 34–61.

[13] Jones, D. E. H. The stability of the bicycle. Physics Today (April 1970): 34–40. (Republished September 2006, pp. 51–56).

[14] Sharp, R. S. The stability and control of motorcycles. <u>Journal of Mechanical Engineering Science</u> 13, 5 (1971) : 316–329.

[15] Sommerfeld, A. <u>Mechanics.</u> New York: Academic, 1952.

[16] Åström, K., Klein, R., and Lennartsson, A. Bicycle dynamics and control: adapted bicycles for education and research. <u>IEEE Control Systems Magazine</u> 25 (August 2005) : 26–47.

[17] TUDelft. <u>History of bicycle steer and dynamics equations,</u> [Online]. Available at http://home.tudelft.nl/en/research/science-projects/delft-bicycle-research/ [2012, April 20]

[18] Chidzonga, R., and Chikuni, E. Stabilizing a bicycle below critical speed. in <u>Proceedings of the African Conference</u>, pp. 1–7, September 2007.

[19] Michini B. and Torrez S. Autonomous Stability Control of a Moving Bicycle. <u>AIAA NE Regional Student Conference</u>, 2007.

[20] Beznos, A., et. al. Control of autonomous motion of two-wheel bicycle with gyroscopic stabilisation. in <u>Proceedings of the IEEE International Conference on Robotics and Automation</u>, vol. 3, pp. 2670–2675, May 1998.

[21] Gallaspy, J. <u>Gyroscopic stabilization of an unmanned bicycle</u>. Master's thesis, Auburn University, 1999.

[22] Karnopp, D. Tilt Control for Gyro-Stabilized Two-Wheeled Vehicles. <u>Vehicle System Dynamics</u> 37 (2002): 145–156.

[23] Keo, L., and Yamakita, M. Dynamic model of a bicycle with a balancer and its control. in <u>Proceedings, Bicycle and Motorcycle Dynamics</u>, Delft, The Netherlands , October 2010.

[24] Guo, L., Liao, Q., and Wei, S. Design of Fuzzy Sliding-mode Controller for Bicycle Robot Nonlinear System. in <u>Proceedings of the IEEE International Conference on Robotics and Biomimetics</u>, pp. 176–180, December 2006.

[25] Yamaguchi, T., Shibata, T., and Murakami, T. Self-Sustaining Approach of Electric Bicycle by Acceleration Control Based backstepping. in <u>Proceedings of the 33rd Annual Conference of the IEEE Industrial Electronics Society</u>, pp. 2610–2614, November 2007.

[26] Guo, L., Liao, Q., Wei, Si., and Zhuang Yi. Design of linear quadratic optimal controller for bicycle robot. in <u>Proceedings of the IEEE International Conference on Automation and Logistics,</u> pp. 1968–1972, August 2009.

[27] Defoort, M., and Murakami, T. Sliding-Mode Control Scheme for an Intelligent Bicycle. <u>IEEE Transactions on Industrial Electronics</u> 56, 9 (September 2009) : 3357–3368.

[28] Bemporad, A., Trecate, G. F., and Morari M. Observability and controllability of piecewise affine and hybrid systems. <u>IEEE Transactions on Automatic Control</u> 45, 10 (October 2000) : 1864–1876.

[29] Schutter, B. D., and Van den Boom, T. J. J. MPC for continuous picewise-affine systems. <u>Systems and Control Letter</u>, vol. 39, no. 8 pp. 697–699, August 1992.

[30] Lin, J. N., and Unbehauen, R. Canonical piecewise-linear approximations. <u>IEEE Transactions on Circuits and Systems I: Fundamental Theory and Applications</u> 39, 8 (August 1992) : 697–699.

[31] Stern, T. E. <u>Piecewise-linear network theory</u> Technical Report. MIT, Cambridge, June 1956.

[32] Katzenelson, J. An algorithm for solving nonlinear resistor networks. <u>The Bell System Technical Journal</u> (October 1965) : 1605–1620.

[33] Chua, L., and Kang, S. M. Section-wise piecewise-linear functions: Canonical representation, properties, and applications. in <u>Proceedings of the IEEE</u>, vol. 65, no. 6, pp. 915–929, June 1977.

[34] Kang, S. M., and Chua, L. O. A global representation of multidimensional piecewise-linear functions with linear partitions. <u>IEEE Transactions on Circuits and Systems</u> 25, 11 (November 1978): 938–940.

[35] Kahlert, C., and Chua, L.O. A generalized canonical piecewise-linear representation. <u>IEEE Transactions on Circuits and Systems</u> 37, 3 (November 1978) : 373–382.

[36] Chua, L. O. Modeling of three terminal devices: a black box approach. <u>IEEE Transactions on Circuits Theory</u> 19, 6 (November 1972) : 555–562.

[37] Chua, L. O., and Deng, A. C. Canonical piecewise-linear modeling. <u>IEEE Transactions on Circuits and Systems</u> 33, 5 (May 1986) : 511–524.

[38] Julian, P., Desages, A., and Agamennoni, O. High-level canonical piecewise linear representation using a simplicial partition. <u>IEEE Transactions on Circuits and Systems I: Fundamental Theory and Applications</u> 46, 4 (April 1999) : 463–480.

[39] Breiman, L. Hinging hyperplanes for regression, classification, and function approximation. <u>IEEE Transactions on Information Theory</u> 39, 3 (May 1993) : 999–1012.

[40] Pucar, P., and Sjöberg, J. On the hinge-finding algorithm for hinging hyperplanes. <u>IEEE Transactions on Information Theory</u> 44, 3 (May 1998) : 1310–1319.

[41] Hush, D. R., and Horne, B. Efficient algorithm for function approximation with piecewise linear sigmoidal networks. <u>IEEE Transactions on Neural Networks</u> 9, 6 (November 1998) : 1129–1140.

[42] Casselman, S., and Rodrigues, L., A new methodology for piecewise affine models using voronoi partitions. in <u>Proceedings of the 48th IEEE Conference on Decision and Control, held jointly with the 28th Chinese Control Conference</u>, pp. 3920–3925, December 2009.

[43] Julian, P., Jordan, M., and Desages, A. Canonical piecewise-linear approximation of smooth functions. <u>IEEE Transactions on Circuits and Systems I: Fundamental Theory and Applications</u> 45, 5 (May 1998) : 567–571.

[44] D'Ambrosio, C., Lodi, A., and Martello, S. Piecewise linear approximation of functions of two variables in MILP models. <u>Operations Research Letters</u>, 38 (2010) : 39–46.

[45] Misener, R., and Floudas, C. A. Piecewise-linear approximations of multidimensional functions. <u>Journal of Optimization Thoery and Applications</u> 145 1 (2010) : 120–147.

[46] Verdult, V., and Verhaegen, M. Subspace identification of piecewise linear system. <u>43rd IEEE Conference on Decision and Control</u>, vol. 4, pp. 3838–3843, December 2004.

[47] Ferrari-Trecate, G., Muselli, M., Liberati, D., and Morari, M. Identification of piecewise affine and hybrid systems. in <u>Proceedings of the American Control Conference</u>, vol. 5, pp. 3521–3526, 2001.

[48] Lai, C. Y., Xiang, C., and Lee, T. H. Identification and control of nonlinear systems via piecewise affine approximation. <u>49th IEEE Conference on Decision and Control</u>, pp. 6395–6402, December 2010.

[49] Juloski, A.Lj., Weiland, S., and Heemels, W.P.M.H. A bayesian approach to identification of hybrid systems. <u>IEEE Transactions on Automatic Control</u> 50, 10 (October 2005) : 1520–1533.

[50] Bemporad, A., Garulli, A., Paoletti, S., and Vicino, A. A bounded-error approach to piecewise affine system identification. <u>IEEE Transactions on Automatic Control</u> 50 (October 2005) : 1567–1580.

[51] Juloski A. Lj., et al. Comparison of four procedures for the identification of hybrid systems. in <u>Hybrid Systems Computation and Control</u>, Springer Verlag, pp. 354–369, 2005.

[52] Paoletti, S., Juloski, A. Lj., Ferrari-Trecate, G., and Vidal, R. Identification of hybrid systems: a tutorial. <u>European Journal of Control</u> (2007) : 242–260.

[53] Sontag, E. D., Nonlinear regulation: the piecewise linear approach. <u>IEEE Transactions on Automatic Control</u> 26, 2 (April 1981) : 346–357.

[54] Juloski, A. Lj., Heemels, W. P. M. H., and Weiland, S. Observer design for a class of piece-wise affine systems. in <u>Proceedings of the 41th IEEE Conference on Decision and Control</u>, pp. 2606–2611, December 2002.

[55] Rodrigues L., and How J. P. Observer-based control of piecewise-affine systems. in <u>Proceedings of the 40th IEEE Conference on Decision and Control</u>, pp. 1366–1371, December 2001.

[56] Heemels, W. P. M. H., Lazar, M., Wouw, N. van de., and Pavlov, A. Observer-based control of discrete-time piecewise affine systems exploiting continuity twice. in <u>Proceedings of the 47th IEEE Conference on Decision and Control</u>, pp. 4675–4680, December 2008.

[57] Hassibi, A., and Boyd, S. Quadratic stabilization and control of piecewise-linear systems. in <u>Proceedings of the 1998 American Control Conference</u>, vol. 6, pp. 3659–3664, June 1998.

[58] Mignone, D., Ferrari-Trecate, G, and Morari, M. Stability and stabilization of piecewise affine and hybrid systems: an LMI approach. in <u>Proceedings of the 39th IEEE Conference on Decision and Control</u>, vol. 1, pp. 504–509, 2000.

[59] Tütüncü, R. H., Toh, K. C., and Todd, M. J. SDPT3 – a Matlab software package for semidefinite programming. <u>Optimization Methods and Software</u>, vol. 11, pp. 545–581 , 1999.

[60] Löfberg, J. <u>YALMIP : A Toolbox for Modeling and Optimization in MATLAB</u>. ETH, [Online], 2004. Available at http://control.ee.ethz.ch/ joloef/yalmip.php.

[61] Rantzer, A., and Johansson, M. Piecewise linear quadratic optimal control. <u>IEEE Transactions on Automatic Control</u> 45 (April 2000) : 629–637.

[62] Johansson, M. <u>Piecewise linear control systems: A computational approach</u>. Germany: Springer-Verlag Berlin Heidelberg, 2003.

[63] Almer, S., Mariethoz, S., and Morari M. Piecewise affine modeling and control of a step-up DC-DC converter. <u>American Control Conference</u>, pp. 3299–3304, July 2010.

[64] Keshavarz, M., Yazdi, M. B., and Jahed-Motlagh, M. R. Piecewise affine modeling and control of a boiler-turbine unit. <u>Applied Thermal Engineering</u> 30 (2010) : 781–791.

[65] Tahami, F., Poshtkouhi, S., and Ahmadian, H. M. Piecewise affine control design for power factor correction rectifiers. <u>Journal of Power Electronics</u> 11 3 (May 2011) : 327–334.

[66] Suntharasantic, S. <u>Piecewise affine control for autonomous bicycle using gyroscopic effect</u>. Master's Thesis, Department of Electrical Engineering, Graduate School, Chulalongkorn University, 2011.

[67] Suntharasantic, S. and Wongsaisuwan, M. Piecewise affine model and control of bicycle by gyroscopic stabilization. in <u>Proceedings of the IEEE Conference on Electrical Engineering/Electronics, Computer, Telecommunications and Information Technology</u>, pp. 549–552, May 2011.

[68] Suntharasantic, S., Rungtweesuk, P., and Wongsaisuwan, M. Piecewise affine model approximation for unmanned bicycle. in <u>Proceedings of IEEE Conference on Instrumentation, Control, Information Technology and System Integration</u>, pp. 1063–1068, September 2011.

[69] Chilali, M., and Gahinet, P. $H_\infty$ design with pole placement constraints: an LMI approach. <u>IEEE Transactions on Automatic Control</u> 41, 3 (March 1996) : 358–367.

[70] Ostertag, E., <u>Mono- and multivariable control and estimation.</u> Springer Heidelberg Dordrecht, 2011.

[71] Satoh, A., and Sugimoto, K. An LMI approach to gain parameter design for regional eigenvalue/eigenstructure assignment. <u>45th IEEE Conference on Decision and Control</u>, pp. 5778–5783, December 2006.

[72] Chang, W., Park, J. B., and Joo, Y. H. LMI approach to digital redesign of linear time-invariant systems. in <u>IEEE Proceedings on Control Theory and applications</u>, vol. 149, no. 4 pp. 297–302, July 2002.

[73] Meijaard, J. P., Papadopoulos, J.M., Ruina, A., and Schwab, A. L. Linearized Dynamics Equations For the Balance and Steer of a Bicycle: A Benchmark and Review. in <u>Proceedings of the Royal Society A: Mathematical, Physical and Engineering Sciences</u>, pp. 1955–1982, August 2007.

[74] Wikipedia. <u>Haversine formula</u>, [Online]. Available at http://en.wikipedia.org/wiki/Haversine_formula [2012, May 20]

**APPENDIX**

# BICYCLE PARAMETERS AND EQUIPMENT SPECIFICATIONS

Table A.1: Parameters for experimental bicycle with gyroscopic flywheel

| Parameter | Symbol | Value | Unit |
|---|---|---|---|
| Bicycle body mass | $m_B$ | 30 | kg |
| Flywheel mass | $m_G$ | 9 | kg |
| Bicycle moment of inertia | $(I_{Bxx}, I_{Byy}, I_{Bzz})$ | (5.947,8.083,2.295) | kg· m$^2$ |
| Flywheel moment of inertia | $(I_{Gxx}, I_{Gyy}, I_{Gzz})$ | (0.138,0.138,0.274) | kg· m$^2$ |
| Height of bicycle center of mass | $z_B$ | 0.49 | m |
| Height of flywheel center of mass | $z_G$ | 0.88 | m |
| Flywheel spinning angular velocity | $\Omega$ | 2000 | rpm |
| Gravitational acceleration | $g$ | 9.81 | m/s$^2$ |
| Bicycle speed | $\sigma$ | 2 | m/s |
| Bicycle wheel base length | $b$ | 1.07 | m |

Table A.2: Parameters for steering motor (Maxon DC motor RE40)

| Parameter | Symbol | Value | Unit |
|---|---|---|---|
| Speed constant | $K_s$ | 581 | rpm/V |
| EMF constant | $K_e$ | 0.0164 | V/rad |
| Torque constant | $K_t$ | 0.0164 | N·m/A |
| Steering viscous damping | $B_{steer}$ | 0 | N·m·s |
| Rotor viscous damping | $B_m$ | 0.0023 | N·m·s |
| Steering inertia | $J_{steer}$ | 0 | kg·m$^2$ |
| Rotor inertia | $J_m$ | $1.35 \times 10^{-5}$ | kg·m$^2$ |
| Terminal resistance | $R_a$ | 0.117 | $\Omega$ |
| Terminal inductance | $L_a$ | $2.45 \times 10^{-5}$ | H |
| Nominal voltage | $V_{max}$ | 12 | V |

**Global Positioning System (GPS)**

We calculate the GPS resolution from the LS20030-3 series GPS module which can measure the latitude and longitude with the resolution $10^{-4}$ minutes parts ($\frac{1}{60} \times 10^{-4}$ degrees). The approximated resolutions in xy-coordinate are obtained by using explicit haversine formula [74]

$$d = 12742000 \arcsin \left( \sqrt{\sin^2 \left( \frac{lat_2 - lat_1}{2} \right) + \cos(lat_1) \cos(lat_2) \sin^2 \left( \frac{lon_2 - lon_1}{2} \right)} \right)$$

where        $d$         is the spherical distance between two points (m)

$lat_1, lat_2$    are the latitudes of two points (rad)

$lon_1, lon_2$    are the longitudes of two points (rad)

# Biography

Mr. Prachya was born in Bangkok, Thailand, in 1988. While in high school, Joseph Upatham, he was granted a full tuition fee scholarship for outstanding students along 6 years. As a highly self-motivated individual, he took a non-degree program of Science, Computer Science in Ramkhamhaeng University when he studied in grade 10. Then he attended a Continuous Bachelor-Master degree program in the department of Electrical Engineering, Chulalongkorn University. He graduated the Bachelor degree of Electrical Engineering at Chulalongkorn University in 2011. He did research in the Control Systems Research Laboratory (CSRL) on a strategic research area of Advanced Control and Optimization and expected to complete Master degree of Electrical Engineering in 2012.

During graduate study, Prachya's research was under the supervision of Assistant Professor Manop Wongsaisuwan. His research interests include the piecewise affine control, nonlinear control, bicycle control and intelligent robotics.

# List of Publications

1. P. Rungtweesuk, and M. Wongsaisuwan. State Feedback Redesign for PWA System with Regional Pole Placement Performance Using LMI. in *Proc. of ECTI-CON conference*. (2012).

2. S. Suntharasantic, P. Rungtweesuk, and M. Wongsaisuwan. Piecewise Affine Model Approximation for Unmanned Bicycle. in *Proc. of SICE Annual Conference*. (2011).